

Jacob Rosen • Blake Hannaford  
Richard M. Satava  
Editors

# Surgical Robotics

Systems Applications and Visions

 Springer

*Editors*

Jacob Rosen  
Department of Computer Engineering  
Jack Baskin School of Engineering  
University of California Santa Cruz  
1156 High Street, Santa Cruz  
CA 95064, USA  
rosen@ucsc.edu

Blake Hannaford  
Department of Electrical Engineering  
University of Washington  
Box 325500, Seattle  
Washington 98195-2500  
USA  
hannaford@ee.washington.edu

Richard M. Satava  
Department of Surgery  
University of Washington Medical Center  
Box 356410  
1959 Pacific Street NE, Seattle  
Washington 98195, USA  
rsatava@u.washington.edu

ISBN 978-1-4419-1125-4                      e-ISBN 978-1-4419-1126-1  
DOI 10.1007/978-1-4419-1126-1  
Springer New York Dordrecht Heidelberg London

© Springer Science+Business Media, LLC 2011

All rights reserved. This work may not be translated or copied in whole or in part without the written permission of the publisher (Springer Science+Business Media, LLC, 233 Spring Street, New York, NY 10013, USA), except for brief excerpts in connection with reviews or scholarly analysis. Use in connection with any form of information storage and retrieval, electronic adaptation, computer software, or by similar or dissimilar methodology now known or hereafter developed is forbidden.

The use in this publication of trade names, trademarks, service marks, and similar terms, even if they are not identified as such, is not to be taken as an expression of opinion as to whether or not they are subject to proprietary rights.

Printed on acid-free paper

Springer is part of Springer Science+Business Media ([www.springer.com](http://www.springer.com))

## Chapter 25

# Objective Assessment of Surgical Skills

Jacob Rosen, Mika Sinanan, and Blake Hannaford

**Abstract** Minimally invasive surgery (MIS) involves a multi-dimensional series of tasks requiring a synthesis between visual information and the kinematics and dynamics of the surgical tools. Analysis of these sources of information is a key step in mastering MIS but may also be used to define objective criteria for characterizing surgical performance. The BlueDRAGON is a new system for acquiring the kinematics and the dynamics of two endoscopic tools synchronized with the visual view of the surgical scene. It includes passive mechanisms equipped with position and force torque sensors for measuring the position and the orientation (P/O) of two endoscopic tools along with the force and torque (F/T) applied on them by the surgeon's hands. The analogy between Minimally Invasive Surgery (MIS) and human language inspires the decomposition of a surgical task into its primary elements in which tool/tissue interactions are considered as "words" that have versions pronunciations defined by the F/T signatures applied on the tissues and P/O of the surgical tools. The frequency of different elements or "words" and their sequential associations or "grammar" both hold critical information about the process of the procedure. Modeling these sequential element expressions using a multi finite states model (Markov model – MM) reveals the structure of the surgical task and is utilized as one of the key steps in objectively assessing surgical performance. The surgical task is modeled by a fully connected, 30 state Markov model representing the two surgical tools where each state corresponds to a fundamental tool/tissue interaction based on the tool kinematics and associated with unique F/T signatures. In addition to the MM objective analysis, a scoring protocol was used by an expert surgeon to subjectively assess the subjects' technical performance. The experimental protocol includes seven MIS tasks performed on an animal

---

© 2006 IEEE. Reprinted, with premission, from "Generalized Approach for Modeling Minimally Invasive Surgery as a Stochastic Process Using a Discrete Markov Model" By Rosen Jacob, Jeffrey D. Brown, Lily Chang, Mika N. Sinanan Blake Hannaford. That was published in: IEEE Transactions on Biomedical Engineering Vol. 53, No. 3, March 2006, pp. 399–413

J. Rosen (✉)

Department of Computer Engineering, Jack Baskin School of Engineering,  
University of California Santa Cruz, 1156 High Street, Santa Cruz, CA 95064, USA  
e-mail: rosen@ucsc.edu

model (pig) by 30 surgeons at different levels of training including expert surgeons. Analysis of these data shows that the major differences between trainees at different skill levels were: (a) the types of tool/tissue interactions being used, (b) the transitions between tool/tissue interactions being applied by each hand, (c) time spent while performing each tool/tissue interaction, (d) the overall completion time, and (e) the variable F/T magnitudes being applied by the subjects through the endoscopic tools. An objective learning curve was defined based on measuring quantitative statistical distance (similarity) between MM of experts and MM of residents at different levels of training. The objective learning curve (e.g. statistical distance between MM) was similar to that of the subjective performance analysis. The MM proved to be a powerful and compact mathematical model for decomposing a complex task such as laparoscopic suturing. Systems like surgical robots or virtual reality simulators in which the kinematics and the dynamics of the surgical tool are inherently measured may benefit from incorporation of the proposed methodology for analysis of efficacy and objective evaluation of surgical skills during training.

**Keywords** Dynamics · Human Machine Interface · Haptics · Kinematics · Manipulation · Markov Model · Minimally Invasive · Simulation · Surgery · Surgical Skill Assessment · Soft Tissue · Surgical Tool · Robotics · Vector Quantization

## 25.1 Introduction

Evaluation of procedural skills in surgery can be performed utilizing three different modalities: during actual open or minimally invasive clinical procedures; in physical or virtual reality simulators with or without haptic feedback; and during interaction with surgical robotic systems (Fig. 25.1). In each of these interactions,

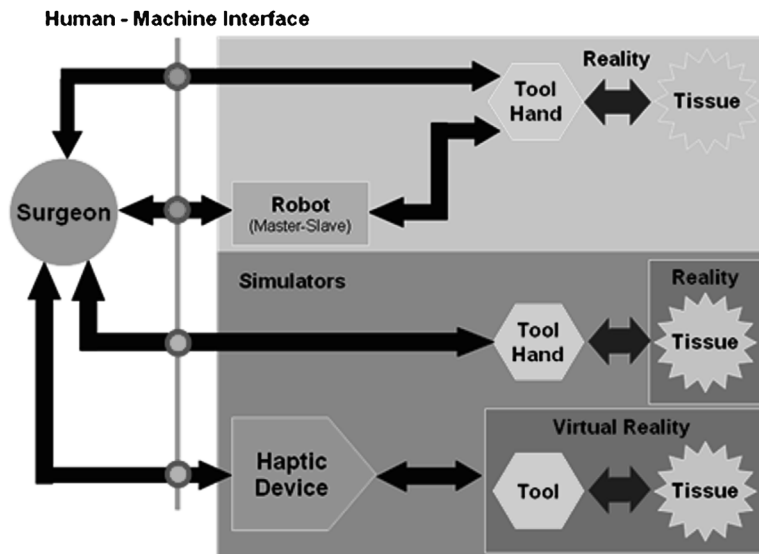


**Fig. 25.1** Modalities for performing surgery

the surgeon is separated from the treated tissue or medium by an instrument, an interface that is at least mechanical, but may be a combination of mechanical and virtual representation of the anatomy (simulator). The intermediate modality in all of these options can be considered interchangeable.

During open or minimally invasive surgical (MIS) procedures, the surgeon interacts with the patient's tissue either directly with his/her hands or through the mediations of tools. Surgical robotics enables the surgeon to operate in a teleoperation mode with or without force feedback using a master/slave system configuration. In this mode of operation, visualization is obtained from either an external camera or an endoscopic camera. Incorporating force feedback, allows the surgeon to feel through the master console the forces being applied on the tissue by the surgical robot, the slave, as he/she interacts with it from the master console. For training in a simulated virtual environment, the surgical tools, the robot – slave, and the anatomical structures are replaced with virtual counterparts. The surgeon interacts with specially-designed input devices, haptic devices when force feedback is incorporated, that emulate surgical tools, or with the master console of the robotic system itself, and perform surgical procedures in virtual reality.

One element that all these modalities have in common is the human-machine interface in which visual, kinematic, dynamic, and haptic information are shared between the surgeon and the various modalities. This interface, rich with multi-dimensional data, is a valuable source of objective information that can be used to objectively assess technical surgical and medical skill within the general framework of surgical and medical ability. Algorithms that are developed for objective assessment of skill are independent of the modality being used, and therefore, the same algorithms can be incorporated into any of these technologies.

Advances in surgical instrumentation have expanded the use of minimally invasive surgical (MIS) techniques over the last decade. Using a miniature video camera and instruments inserted through small incisions, operations previously performed through large incisions are now completed with MIS techniques leading to a much shorter recovery time and decreased risk of surgical site infections. However from surgeon's perspective, this new technology requires a new set of skills. The new human-machine interface, the associated loss of 3-D vision, and degraded haptic sensation introduce new challenges. Moreover, the use of this technology has also presented a new dilemma – namely the training of individuals to perform surgical procedures that require a new set of skills. This is especially problematic in the field of MIS where the teacher is one step removed from the actual conduct of the operation.

Developing objective methodology for surgical competence and performance are paramount to superior surgical training. Moreover, alternatives to the traditional apprenticeship model of surgical training are necessary in today's emphasis on cost containment and professional competency and patient safety. There is a need to demonstrate continuing competency among practicing surgeons as well as confirming competency in trainees early on, before surgical trainees are thrust into the role of primary assistant or surgeon in the operating room. Inherent difficulties in evaluating clinical competence for physicians and physicians-in-training have spawned the wide

use of various assessment techniques including Objective Structured Clinical Examinations (OSCE), oral examinations, standardized patient examinations, and simulation technology. While successful evaluation of cognitive skills using these methods have been reported, objective evaluation of procedural skills remains difficult. As the medical profession is faced with demands for greater accountability and patient safety, there is a critical need for the development of consistent and reliable methods for objective evaluation of clinician performance during procedures.

Objective assessment of surgical competence during MIS procedures, defined as caring out the surgical procedure in a minimally invasive surgical setup, is a multi-dimensional problem. MIS performance is comprised of physiological constraints (stress fatigue) equipment constraints (camera rotation and port location), team constraints (nurses) and MIS ability. Ability when referred to surgery, is defined as the natural state or condition of being capable; innate aptitude (prior to training) which an individual brings for performing a surgical task [1]. MIS ability, by itself, includes cognitive factors (knowledge and judgment) and technical factors (psychomotor ability, visio-spatial ability and perceptual ability). By definition, fundamental psychometric abilities are fixed at birth or early childhood and show little or no learning effect [2]. However training enables the subject to perform as close as possible to his or her inherent psychometric abilities.

The methodology for assessing surgical skill as a subset of surgical ability, is gradually shifting from subjective scoring of an expert which may be a variably biased opinion using vague criteria, towards a more objective, quantitative analysis. This shift is enabled by using instrumented tools [3–7], measurements of the surgeon's arm kinematics [8], gaze patterns [9], physical simulators [10], a variety of virtual reality simulators with and without haptics [1, 11–32], and robotic systems. Regardless of the modality being used or the clinical procedure being studied, task deconstruction or decomposition is an essential component of a rigorous objective skills-assessment methodology. By exposing and analyzing the internal hierarchy of tasks a broader understanding of procedures is achieved while providing objective means for quantifying training and skills acquisition.

Task decomposition is associated with defining the prime elements of the process. In surgery, a procedure is traditionally and methodologically divided into steps, stages, or phases with well-defined intermediate goals. Additional hierarchical decomposition is based upon identifying tasks or subtasks [33] composed of sequence of and actions or states [3–7]. In addition, other measurable parameters such as workspace [34] completion time, tool position, and forces and torques were studied individually [3–7]. Selecting low-level elements of the task decomposition allows one to associate these elements with quantifiable and measurable parameters. The definition of these states, along with measurable, quantitative data, are the foundation for modeling and examining surgical tasks as a process.

In the current study, an analogy between (MIS) and the human language inspires the decomposition of a surgical task into its primary elements. Modeling the sequential element expressions using a multi states model (Markov model) reveals the internal structure of the surgical task, and this is utilized as one of the key steps in objectively assessing surgical performance. Markov Modeling (MM) and its

subset – Hidden Markov Modeling (HMM) were extensively developed in the area of speech recognition [35] and further used in a broad spectrum of other fields, e.g. human operator modeling, robotics, and teleoperation [36–40], gesture recognition and facial expressions [41, 42] DNA and protein modeling [43], and surgical tools in MIS setup [5, 44]. These studies indicate that MMs and HMMs provide adequate models to characterize humans operating in complex interactive tasks with machines among other applications.

The aim of the study was to develop a system of acquiring data in a real MIS setup using an animal model and a methodology for decomposing two-handed surgical tasks using Markov models (MM) based on the kinematics and the dynamics of the surgical tools. Measuring the statistical similarity between the models representing subjects at different levels of their surgical training enables an objective assessment of surgical skills.

## 25.2 Tools and Methods

A novel system named the BlueDRAGON was designed, constructed and used for acquiring the kinematics (position and orientation) and the dynamics (force and torque) of two endoscopic tools during MIS procedures in real-time. The data were acquired during a surgical task performed by 30 subjects at different levels of surgical training followed by objective and subjective surgical skill analysis based on task decomposition. The novel objective methodology was based upon a multi-state Markov model whereas the subjective methodology utilized a standard scoring system for analyzing the videotapes of the surgical scene recorded during the experiment. The following subsections describe the system and the methodologies that were used in the current study.

### 25.2.1 Tools: *The BlueDRAGON System*

The BlueDRAGON is a system for acquiring the kinematics and the dynamics of two endoscopic tools along with the visual view of the surgical scene while performing a MIS procedure (Fig. 25.2). The system includes two four-bar passive mechanisms attached to endoscopic tools [4]. The endoscopic tool in minimal invasive surgery is inserted into the body through a port located for example in the abdominal wall. The tool is rotated around a pivot point within the port that is inaccessible for sensors aimed to measure the tool's rotation. The four bar mechanism is one of several mechanisms that allows mapping of the tool's rotation around the port's pivot point. This mapping is enabled by aligning a specific point on the mechanism, where all its rotation axes are intersecting, with the pivot point of the endoscopic tool (Fig. 25.2b). The tool's positions and orientations, with respect to the port, are then tracked by sensors that are incorporated into the mechanism's joints. Moreover,

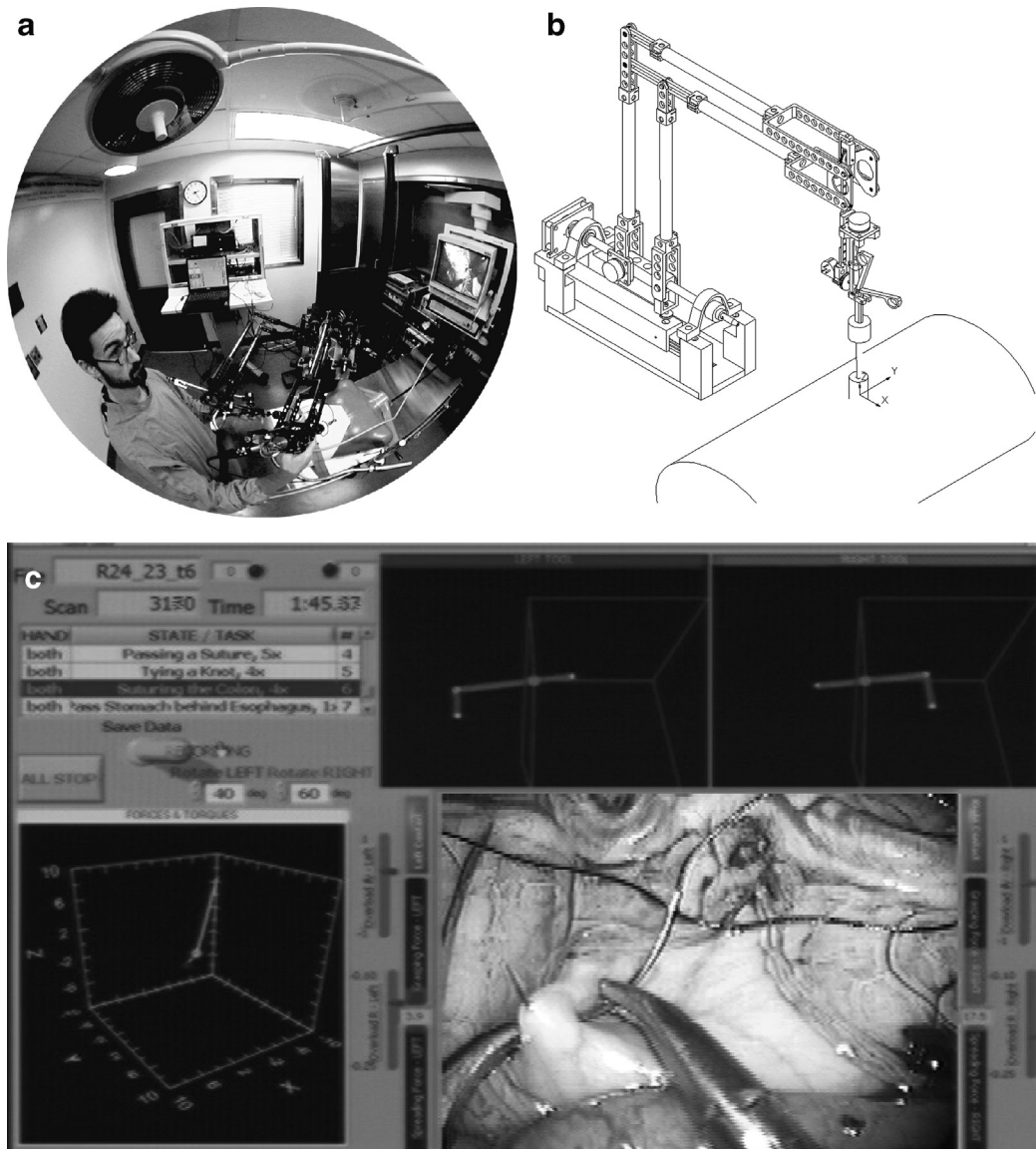


**Fig. 25.2** The BlueDRAGON system (a) The system integrated into a minimally invasive surgery operating room (b) CAD drawing of the BlueDRAGON four bar mechanism and its coordinate system properly aligned with the MIS port. (c) Graphical user interface (GUI) incorporating visual view of the surgical seen acquired by the endoscopes video camera (*bottom right*) and real-time information measured by the BlueDRAGONS. On the top right side of the GUI, a virtual representation of the two endoscopic tools are shown along with vectors representing the instantaneous velocities. On the *bottom left* a three dimensional representation of the forces and torque vectors are presented. Surrounding the endoscopic image are *bars* representing the grasping/spreading forces applied on the handle and transmitted to the tool tip via the tool's internal mechanism, along with virtual binary LED indicating contact between the tool tips and the tissues

the mechanism's axes alignment with the pivot point in the port prevents the application of additional moments applied on the skin and internal tissues that may result from misalignment and the fact that an external mechanism is used and

attached to the tools. On the other hand, this setup makes the mechanism totally transparent to the moments that are generated intentionally by using the tools.

Substantial effort was made, during the design process, to minimize the weight and the inertia of the mechanism. This was accomplished by using carbon fibers tubes for the links, and by optimizing the shapes of the links for minimizing the mass distribution. The mass of the mechanism's moving parts is 1.36 kg and its maximal moment of inertia relative to the X-axis ( $I_{xx}$ ) depicted in Fig. 25.2b is 0.157 kg m<sup>2</sup>. Moreover, the gravitational forces applied on the surgeon's hand when the mechanism is placed away from its neutral position are compensated by an optimized spring connecting the base with the first two coupled links.

The two mechanisms are equipped with three classes of sensors: (a) position sensors (potentiometers – Midori America Corp.) are incorporated into four of the mechanisms' joints for measuring the position, the orientation and the translation of the two instrumented endoscopic tools attached to them. In addition, two linear potentiometers (Penny & Giles Controls Ltd.) that are attached to the tools' handles are used for measuring the endoscopic handle and tool tip angles; (b) three-axis force/torque (F/T) sensors with holes drilled at their center (ATI-Mini sensor) are inserted and clamped to the proximal end of the endoscopic tools' shafts. In addition, double beam force sensors (Futak) were inserted into the tools' handles for measuring the grasping forces at the hand/tool interface; and (c) contact sensors, based on RC circuit, provided binary indication of any tool-tip/tissue contact.

Data measured by the BlueDRAGON sensors are acquired using two 12-bit USB A/D cards (National Instruments) sampling the 26 channels (four rotations, one translation, one tissue contact, and seven channels of forces and torques from each instrumented grasper) at 30 Hz. In addition to the data acquisition, the synchronized view of the surgical scene is incorporated into a graphical user interface displaying the data in real-time (Fig. 25.2c).

### **25.2.2 Experimental Protocol**

The experimental protocol included 30 surgeons at different levels of expertise from surgeons in training to surgical attendings skilled in laparoscopic surgery. There were five subjects in each group representing the 5 years of surgical training, (5 × R1, R2, R3, R4, R5 – where the numeral denotes year of training) and five expert surgeons. Each subject was given instruction on how to perform an intracorporeal knot through a standard multimedia presentation. The multimedia presentation included a written description of the task along with a video clip of the surgical scene and audio explanation of the task. Subjects were then given a maximum of 15 min to complete this task in a swine model. This complex, integrative task includes many of the elements of advanced MIS techniques.

In addition to the surgical task, each subject performed 15 predefined tool/tissue and tool/needle-suture interactions (Table 25.1). The kinematics (the position/

**Table 25.1** Definitions of the 15 states based on spherical coordinate system with an origin at the port

Type	No.	State name	State acronym	Tissue contact	Position/Orientation	Force/Torque
I	1	Idle	ID	-	$\omega_x \pm \varepsilon_{\omega_x}$	$F_x \pm \varepsilon_{F_x}$
	2	Closing Handle (Grasping/ Cutting)	CL	+	$\omega_y \pm \varepsilon_{\omega_y}$ $\omega_z \pm \varepsilon_{\omega_z}$ $v_r \pm \varepsilon_{v_r}$ $\omega_g < \varepsilon_{\omega_g}$ $\pm \varepsilon_{\omega_x}$	$F_y \pm \varepsilon_{F_y}$ $F_z \pm \varepsilon_{F_z}$ $T_x \pm \varepsilon_{T_x}$ $T_y \pm \varepsilon_{T_y}$ $T_z \pm \varepsilon_{T_z}$ $F_g > \varepsilon_{F_g}$
	3	Opening Handle (Spreading)	OP	+	$\omega_y \pm \varepsilon_{\omega_y}$ $\omega_z \pm \varepsilon_{\omega_z}$ $v_r \pm \varepsilon_{v_r}$ $\omega_g > \varepsilon_{\omega_g}$	$F_y \pm \varepsilon_{F_y}$ $F_z \pm \varepsilon_{F_z}$ $T_x \pm \varepsilon_{T_x}$ $T_y \pm \varepsilon_{T_y}$ $T_z \pm \varepsilon_{T_z}$ $F_g < -\varepsilon_{F_g}$
	4	Pushing	PS	+	$\omega_x \pm \varepsilon_{\omega_x}$ $\omega_y \pm \varepsilon_{\omega_y}$ $\omega_z \pm \varepsilon_{\omega_z}$ $v_r < -\varepsilon_{v_r}$	$F_x > \varepsilon_{F_x}$ $F_y > \varepsilon_{F_y}$ $F_z > \varepsilon_{F_z}$ $T_x \pm \varepsilon_{T_x}$ $T_y \pm \varepsilon_{T_y}$ $T_z \pm \varepsilon_{T_z}$ $F_g \pm \varepsilon_{F_g}$
	5	Rotating	RT	+	$\omega_x >  \varepsilon $ $\omega_y \pm \varepsilon_{\omega_y}$ $\omega_z \pm \varepsilon_{\omega_z}$ $v_r \pm \varepsilon_{v_r}$	$F_x >  \varepsilon_{F_x} $ $F_y >  \varepsilon_{F_y} $ $F_z \pm \varepsilon_{F_z}$ $T_x >  \varepsilon_{T_x} $ $T_y < \varepsilon_{T_y}$ $T_z \pm \varepsilon_{T_z}$ $F_g \pm \varepsilon_{F_g}$
	6	Closing – Pulling	CL-PL	+	$\omega_x \pm \varepsilon_{\omega_x}$ $\omega_y \pm \varepsilon_{\omega_y}$ $\omega_z \pm \varepsilon_{\omega_z}$ $v_r > \varepsilon_{v_r}$	$F_x \pm \varepsilon_{F_x}$ $F_y \pm \varepsilon_{F_y}$ $F_z < -\varepsilon_{F_z}$ $T_x \pm \varepsilon_{T_x}$ $T_y \pm \varepsilon_{T_y}$ $T_z \pm \varepsilon_{T_z}$ $F_g > \varepsilon_{F_g}$
II	7	Closing – Pulling	CL-PS	+	$\omega_x \pm \varepsilon_{\omega_x}$ $\omega_y \pm \varepsilon_{\omega_y}$ $\omega_z \pm \varepsilon_{\omega_z}$ $v_r < -\varepsilon_{v_r}$	$F_x \pm \varepsilon_{F_x}$ $F_y \pm \varepsilon_{F_y}$ $F_z > \varepsilon_{F_z}$ $T_x \pm \varepsilon_{T_x}$ $T_y \pm \varepsilon_{T_y}$ $T_z \pm \varepsilon_{T_z}$ $F_g > \varepsilon_{F_g}$
	8	Closing – Pulling	CL-RT	+	$\omega_x >  \varepsilon_{\omega_x} $ $\omega_y >  \varepsilon_{\omega_y} $ $\omega_z \pm \varepsilon_{\omega_z}$ $v_r \pm \varepsilon_{v_r}$	$F_x >  \varepsilon_{F_x} $ $F_y >  \varepsilon_{F_y} $ $F_z \pm \varepsilon_{F_z}$ $T_x \pm \varepsilon_{T_x}$ $T_y \pm \varepsilon_{T_y}$ $T_z \pm \varepsilon_{T_z}$ $F_g > \varepsilon_{F_g}$
	9	Pushing – Opening	PS-OP	+	$\omega_x \pm \varepsilon_{\omega_x}$ $\omega_y \pm \varepsilon_{\omega_y}$ $\omega_z \pm \varepsilon_{\omega_z}$ $v_r < \varepsilon_{v_r}$	$F_x \pm \varepsilon_{F_x}$ $F_y \pm \varepsilon_{F_y}$ $F_z < -\varepsilon_{F_z}$ $T_x \pm \varepsilon_{T_x}$ $T_y \pm \varepsilon_{T_y}$ $T_z \pm \varepsilon_{T_z}$ $F_g < -\varepsilon_{F_g}$
	10	Pushing – Rotating	PS-RT	+	$\omega_x >  \varepsilon_{\omega_x} $ $\omega_y \pm \varepsilon_{\omega_y}$ $\omega_z \pm \varepsilon_{\omega_z}$ $v_r < \varepsilon_{v_r}$	$F_x >  \varepsilon_{F_x} $ $F_y \pm \varepsilon_{F_y}$ $F_z > \varepsilon_{F_z}$ $T_x >  \varepsilon_{T_x} $ $T_y \pm \varepsilon_{T_y}$ $T_z \pm \varepsilon_{T_z}$ $F_g \pm \varepsilon_{F_g}$
	11	Rotating – Opening	RT-OP	+	$\omega_x >  \varepsilon_{\omega_x} $ $\omega_y >  \varepsilon_{\omega_y} $ $\omega_z \pm \varepsilon_{\omega_z}$ $v_r < \varepsilon_{v_r}$	$F_x >  \varepsilon_{F_x} $ $F_y >  \varepsilon_{F_y} $ $F_z \pm \varepsilon_{F_z}$ $T_x >  \varepsilon_{T_x} $ $T_y >  \varepsilon_{T_y} $ $T_z \pm \varepsilon_{T_z}$ $F_g < -\varepsilon_{F_g}$
	12	Closing – Pulling	CL-PL-RT	+	$\omega_x >  \varepsilon_{\omega_x} $ $\omega_y >  \varepsilon_{\omega_y} $ $\omega_z \pm \varepsilon_{\omega_z}$ $v_r < -\varepsilon_{v_r}$	$F_x >  \varepsilon_{F_x} $ $F_y >  \varepsilon_{F_y} $ $F_z < -\varepsilon_{F_z}$ $T_x >  \varepsilon_{T_x} $ $T_y >  \varepsilon_{T_y} $ $T_z \pm \varepsilon_{T_z}$ $F_g > \varepsilon_{F_g}$
III	13	Rotating Closing – Pushing –	CL-PS-RT	+	$\omega_x >  \varepsilon_{\omega_x} $ $\omega_y >  \varepsilon_{\omega_y} $ $\omega_z \pm \varepsilon_{\omega_z}$ $v_r < -\varepsilon_{v_r}$	$F_x >  \varepsilon_{F_x} $ $F_y >  \varepsilon_{F_y} $ $F_z \pm \varepsilon_{F_z}$ $T_x >  \varepsilon_{T_x} $ $T_y >  \varepsilon_{T_y} $ $T_z \pm \varepsilon_{T_z}$ $F_g > \varepsilon_{F_g}$
	14	Pushing – Rotating	PS-RT-OP	+	$\omega_x >  \varepsilon_{\omega_x} $ $\omega_y >  \varepsilon_{\omega_y} $ $\omega_z \pm \varepsilon_{\omega_z}$ $v_r < -\varepsilon_{v_r}$	$F_x >  \varepsilon_{F_x} $ $F_y >  \varepsilon_{F_y} $ $F_z > \varepsilon_{F_z}$ $T_x >  \varepsilon_{T_x} $ $T_y >  \varepsilon_{T_y} $ $T_z \pm \varepsilon_{T_z}$ $F_g < -\varepsilon_{F_g}$
	15	Closing Handle – Spinning	CL-SP	+	$\omega_x \pm \varepsilon_{\omega_x}$ $\omega_y \pm \varepsilon_{\omega_y}$ $\omega_z > \varepsilon_{\omega_z}$ $ \omega_z  > \varepsilon_{\omega_z}$ $\pm \varepsilon_{v_r}$	$F_x \pm \varepsilon_{F_x}$ $F_y \pm \varepsilon_{F_y}$ $F_z > \varepsilon_{F_z}$ $T_x \pm \varepsilon_{T_x}$ $T_y \pm \varepsilon_{T_y}$ $T_z >  \varepsilon_{T_z} $ $F_g > \varepsilon_{F_g}$

Each state is characterized by a unique set of angular/linear velocities, forces and torques and associated with a specific tool/tissue or tool/object interaction. A non-zero threshold value is defined for each parameter by  $\varepsilon$ . The states' definitions are independent from the tool tip being used e.g. the state defined as Closing Handle might be associated with grasping or cutting if a grasper or scissors are being used respectively

orientation – P/O of the tools in space with respect to the port) and the dynamics (forces and torque F/T applied by the surgeons on the tools) of the left and right endoscopic tools along with the visual view of the surgical scene were acquired by a passive mechanism that is part of the BlueDRAGON. The aim of this experimental segment was to study the F/T and velocity signatures associated with each interaction that were further used as the model observations associated with each state of the model. All animal procedures were performed in an AALAC-accredited surgical research facility under an approved protocol from the institutional animal care committee of the University of Washington.

### 25.2.3 *Objective Analysis: MIS Task Decomposition and Markov Model*

#### 25.2.3.1 *Surgery as a Language: The Analogy and The State Definitions*

The objective methodology for assessing skill while performing a procedure is inspired by the analogy between the human language and surgery. Further analysis of this concept indicates that these two domains share similar taxonomy and internal etymological structure that allows a mathematical description of the process by using quantitative models. Such models can be further used to objectively assess skill level by revealing the internal structure and dynamics of the process. This analogy is enhanced by the fact that in both the human language and in surgery, an idea can be expressed and a procedure can be performed in several different ways while retaining the same cognitive meaning or outcome. This fact suggests that a stochastic approach might describe the surgical or medical examination processes incorporating the inherent variability better than a determinist approach.

Table 25.2 summarizes the analogy between the two entities, human language and surgery, along with the corresponding modeling elements in a hierarchal fashion. The critical step in creating such an analogy is to identify the prime elements. In the human language, the prime element is the ‘*word*’ which is analogous to a ‘*tool/tissue interaction*’ in surgery. This prime element is modeled by a ‘*state*’ in the model. As in a spoken language, words have different ‘*pronunciations*’ and yet preserve their meaning. In surgery, various ‘*force/torque*

**Table 25.2** The analogy between the human language and surgery as manifested it self in a similar taxonomy and sub structures along with the corresponding element of the finite state Markov model

Language	Surgery	Model
Book	Operation/Procedure	Multiple Models
Chapter	Step of the Operation	Model
Word	Tool/Tissue Interaction	State
Pronunciation	Force Torque Velocity magnitude	Observation

*magnitudes*' can be applied on the tissues and still be classified under the same tool/tissue interaction category. These various force/torque magnitudes are simulated by the '*observations*' in the model. In a similar fashion to the human language in which a sequence of words are comprised into a sentence, and sentences create a book '*chapter*', a sequence to tool/tissue interactions form a step of an operation in which an intermediate and specific outcome can be completed. Each step of the operation is represented by a single model. '*Multiple models*' can be further describing a multi-step '*surgical operation*' that is analogous to a '*book*'. One may note that the sub-structures like a sentence and a section were omitted in the current analogy; however, identifying the corresponding elements in surgical procedure may increase the resolution of the model.

Analyzing the degrees of freedom (DOF) of a tool in MIS indicates that the due to the introduction of the port through which the surgeon inserts tools into the body cavity, two DOF of the tool are restricted. The six DOF of a typical open surgical tool is reduced to only four DOF in a minimally invasive setup (Fig. 25.3). These four DOF include rotation along the three orthogonal axes (x,y,z) and translation along the long axis of the tool's shaft (z). A fifth DOF is defined as the tool-tip jaws angle, which is mechanically linked to the tool's handle, when a grasper or a scissor is used. Additional one or two degrees of freedom can be obtained by adding a wrist joint to the MIS tool. The wrist joint has been incorporated into commercially available surgical robots in order to enhance the dexterity of the tool within the body cavity.

Surgeons, while performing MIS procedures, utilize various combinations of the tools' DOF while manipulating them during the interaction with the tissues or other items in the surgical scene (needle, suture, staple etc.) in order to achieve the desire outcome. Quantitative analysis of the tool's position and ordination during surgical procedures revealed 15 different combinations of the tool's five DOF, while interacting with the tissues and other objects. These 15 DOF combinations will be further referred to, and modeled as states (Table 25.1). The 15 states can be grouped into three types, based on the number of movements or DOF utilized simultaneously. The fundamental maneuvers are defined as Type I. The 'idle' state was defined as moving the tool in space (body cavity) without touching any internal organ, tissue, or any other item in the scene. The forces and torques developed in this state represent the interaction with the port and the abdominal wall, in addition to the gravitational and inertial forces. In the 'grasping' and 'spreading' states, compression and tension were applied on the tissue through the tool tip by closing and opening the grasper's handle, respectively. In the 'pushing' state, the tissue was compressed by moving the tool along the Z axis. 'Sweeping' consisted of placing the tool in one position while rotating it around the X and/or Y axes or in any combination of these two axes (port frame). The rest of the tool/tissue interactions in Types II and III were combinations of the fundamental ones defined as Type I. The only one exception was state 15 that was observed only in tasks involved suturing when the surgeon grasps the needle and rotates it around the shaft's long axis to insert it into the tissue. Such a rotation was never observed whenever direct tissue interaction was involved.

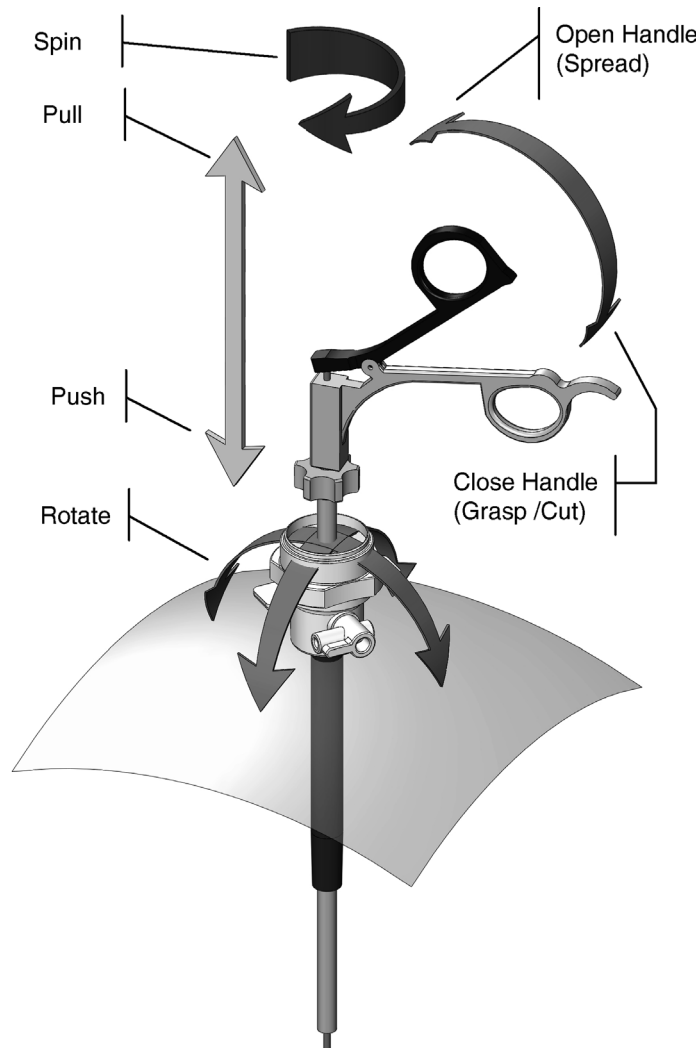


**Fig. 25.3** Definition of the five degrees of freedom – DOF (marked by *arrows*) of a typical MIS endoscopic tool. Note that two DOF were separated into two distinct actions (Open/Close handle and Pull/Push), and the other two were lumped into one action (Rotate) for representing the tool tip tissue interactions (omitted in the illustration). The terminology associated with the various DOF corresponds with the model state definitions (Table 25.1)

### 25.2.3.2 Vector Quantization (VQ)

Each one of the 15 states was associated with a unique set of forces, torques angular and linear velocities, as indicated in Table 25.2. Following the language analogy, in the same way as a word is correlated to a state may be pronounced differently and still retains the same meaning, the tool might be in a specific state while infinite combinations of force, torque angular and linear velocities may be used. A significant data reduction was achieved by using a clustering analysis in a search for discrete number of high concentration cluster centers in the database for each one of the 15 states. As part of this process, the continuous 12 dimensional vectors were transformed into one dimensional vector of 150 symbols (ten symbols for each state).

The data reduction was performed in three phases. During the first phase a subset of the database was created appending all the 12 dimensional vectors associated with each state measured by the left and the right tools and performed by all the subjects (see Sect. 25.2.2 for details). The 12 dimensional subset of the database  $(\dot{\theta}_x, \dot{\theta}_y, \dot{\theta}_z, \dot{\theta}_g, F_x, F_y, F_z, T_x, T_y, T_z, F_g)$  was transformed into a 9 dimensional vector  $(\dot{\theta}_{xy}, \dot{\theta}_z, \dot{\theta}_g, F_{xy}, F_z, T_{xy}, T_z, F_g)$  by calculating the magnitude of the angular velocity, and the forces and torques in the XY plane. This process canceled out differences between surgeons due to variations in position relative to the animal and allowed use of the same clusters for the left and the right tools.

As part of the second phase, a K-means vector quantization algorithm [48] was used to identify ten cluster centers associated with each state. Given  $M$  patterns  $\bar{X}_1, \bar{X}_2, \dots, \bar{X}_M$  contained in the pattern space  $\bar{S}$ , the process of clustering can be formally stated as seeking the regions  $\bar{S}_1, \bar{S}_2, \dots, \bar{S}_K$  such that every data vector  $\bar{X}_i$  ( $i = 1, 2, \dots, M$ ) falls into one of these regions and no  $\bar{X}_i$  is associated in two regions, i.e.

$$\begin{aligned} \bar{S}_1 \cup \bar{S}_2 \cup \bar{S}_3 \dots \cup \bar{S}_K &= \bar{S} \quad (\text{a}) \\ \bar{S}_i \cap \bar{S}_j &= 0 \quad \forall i \neq j \quad (\text{b}) \end{aligned} \quad (25.1)$$

The K-means algorithm, is based on minimization of the sum of squared distances from all points in a cluster domain to the cluster center,

$$\min \sum_{X \in S_j(k)} (\bar{X} - \bar{Z}_j)^2 \quad (25.2)$$

where  $S_j(k)$  was the cluster domain for cluster centers  $\bar{Z}_j$  at the  $k$ th iteration, and  $\bar{X}$  was a point in the cluster domain.

The pattern spaces  $\bar{S}$  in the current study were composed from the F/T applied on the surgical tool by the surgeon along with the tool's angular and linear velocities for different states. A typical data vector  $\bar{X}_i$ , was a 9 dimensional vector defined as  $\{\dot{\theta}_{xy}, \dot{\theta}_z, \dot{\theta}_g, F_{xy}, F_z, T_{xy}, T_z, F_g\}$ . The cluster regions  $\bar{S}_i$  represented by the cluster centers  $\bar{Z}_j$ , defined typical signatures or codeword (pronunciations in the human language realm) associated with a specific state (e.g. PS, PL, GR etc.). The number of clusters identified in each type of state was based upon the squared error distortion criterion (25.3). As the number of clusters increased, the distortion decreased exponentially. Following this behavior, the number of clusters was constantly increased until the squared error distortion gradient as a function of  $k$  decreased below a threshold of 1% that results in ten cluster centers for each state.

$$d(\bar{X}, \bar{Z}) = \|\bar{X} - \bar{Z}_j\|^2 = \sum_{i=1}^k (\bar{X} - \bar{Z}_i)^2 \quad (25.3)$$

In the third phase, the ten cluster centers  $\bar{Z}_j$  for each state (Table 25.2) forming a codebook of 150 discrete symbols were then used to encode the entire database of

the actual surgical tasks converting the continuous multi-dimensional data into a one-dimensional vector of finite symbols. This step of the data analysis was essential for using the discrete version of Markov Model.

### 25.2.3.3 Markov Model (MM)

The final step of the data analysis was to develop a model that represents the process of performing MIS along with the methodology for objectively evaluating surgical skill. The Markov Model was found to be a very compact statistical method to summarize a relatively complex task such as a step or a task of a MIS procedure. Moreover, the skill level was incorporated into the MM by developing different MMs based on data acquired for different levels of expertise starting from a first year residents up to a level of expert surgeons.

The modeling approach underling the methodology for decomposing and statistically representing a surgical task is based on a fully connected, symmetric 30 states MM where the left and the right tools are represented by 15 states each (Fig. 25.4). In view of this model, any MIS task may be described as a series of states. In each state, the surgeon is applying a specific force/torque/velocity signature, out of ten signatures that are associated with that state, on the tissue or on any other item in the surgical scene by using the tool. The surgeon may stay within same state for specific time duration using different signatures associated with that state and then perform a transition to another state. The surgeon may utilize any of the 15 states by using the left and the right tools independently. However, the states representing the tool/tissue or tool/object interactions of the left and the right tools are mathematically and functionally linked.

The MM is defined by the compact notation in (25.4). Each Markov sub-model representing the left and the right tool is defined by  $\lambda_L$  and  $\lambda_R$  (25.4). The sub model is defined by: (a) The number of states  $-N$  whereas individual states are denoted as  $S = \{s_1, s_1, \dots, s_N\}$ , and the state at time  $t$  as  $q_t$

(b) The number of distinct (discrete) observation symbol  $-M$  whereas individual symbols are denoted as  $V = \{v_1, v_1, \dots, v_M\}$

(c) The state transition probability distribution matrix indicating the probability of the transition from state  $q_t = s_i$  at time  $t$  to state  $q_{t+1} = s_j$  at time  $t + 1$  -  $A = \{a_{ij}\}$ , where  $a_{ij} = P[q_{t+1} = s_j | q_t = s_i] \ 1 \leq i, j \leq N$ .

Note that  $A = \{a_{ij}\}$  is a non-symmetric matrix ( $a_{ij} \neq a_{ji}$ ) since the probability of performing a transition from state  $i$  to state  $j$  using each one of the tools is different from the probability of performing a transition from state  $j$  to state  $i$ .

(d) The observation symbol probability distribution matrix indicating the probability of using the symbol  $v_k$  while staying at state  $s_j$  at time  $t$  -  $B = \{b_j(k)\}$ , where for state  $j$   $b_j(k) = P[v_k \text{ at } t | q_t = s_j] \ 1 \leq j \leq N, \ 1 \leq k \leq M$ .

(e) The initial state distribution vector indicating the probability of starting the process with state  $s_i$  at time  $t = 1$  -  $\pi$  where  $\pi_i = P[q_1 = s_i] \ 1 \leq i \leq N$ .

The two sub models are linked to each other by the left-right interstate transition probability matrix or the cooperation matrix indicating the probability for staying

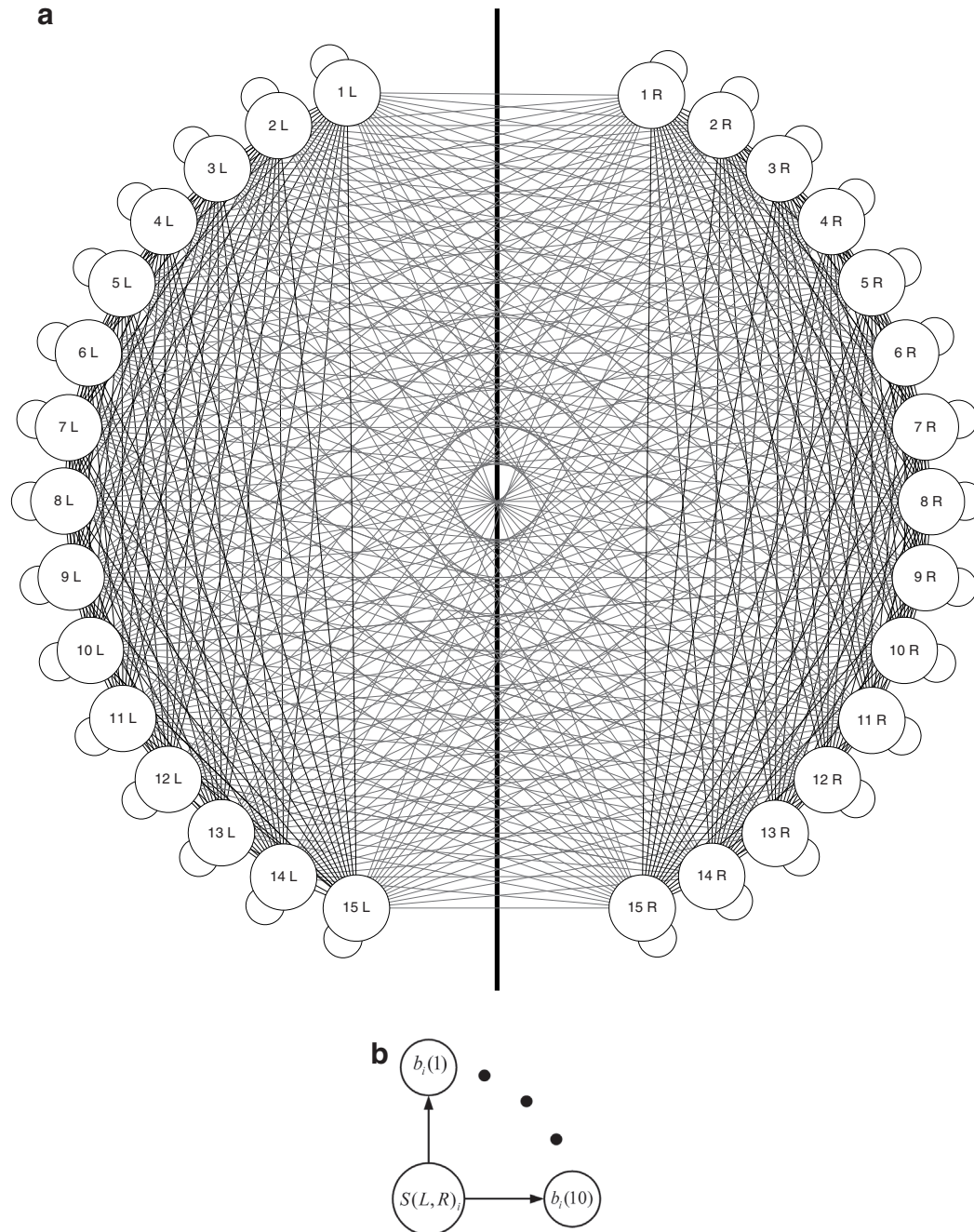


**Fig. 25.4** Finite State Diagrams (FSD) – (a) Fully connected FSD for decomposing MIS. The tool/tissue and tool/object interactions of the left and the right endoscopic tools are represented by the 15 fully connected sub-models. *Circles* represent states whereas *lines* represent transitions between states. Each *line*, that does not cross the *center-line*, represents probability value defined in the state transition probability distribution matrix  $A = \{a_{ij}\}$ . Each *line* that crosses the *center-line*, represents probability for a specific combination of the left and the right tools and defined by the interstate transition probability distribution matrix, or the cooperation matrix  $C = \{c_{lr}\}$ . Note that since the probability of performing a transition from state  $i$  to state  $j$  by each one of the tools is different from probability of performing a transition from state  $j$  to state  $i$ , these two probabilities should have been represented by two parallel lines connecting state  $i$  to state  $j$  and representing the

in states  $s_l$  with the left tool  $s_r$  with the right tool at time  $t$   $-C = \{c_{lr}\}$ , where  $c_{lr} = P[q_{lL} = s_l \cup q_{rR} = s_r] \quad 1 \leq l, r \leq N$

Note that  $C = \{c_{lr}\}$  is a non-symmetric matrix  $c_{lr} \neq c_{rl}$  since it representing the combination of using two states simultaneously by the left and the right tools.

The probability of observing the state transition  $Q = \{q_1, q_2, \dots, q_T\}$  and the associated observation sequence  $O = \{o_1, o_2, \dots, o_T\}$ , given the two Markov sub models (25.4) and interstate transition probability matrix, is defined by (25.5)

$$\lambda_L = (A_L, B_L, \pi_L) \quad \lambda_R = (A_R, B_R, \pi_R) \quad (25.4)$$

$$P(Q, O | \lambda_L, \lambda_R, C) = \pi_{q_L} \pi_{q_R} \prod_{t=0}^T a_{q_t, q_{t+1}L} b_{q_tL}(o_t) a_{q_t, q_{t+1}R} b_{q_tR}(o_t) c_{q_{tL}q_{tR}} \quad (25.5)$$

Since probabilities by definition have numerical value in the range of 0–1, for a relatively short time duration, the probability calculated by (25.5) converges exponentially to zero; and therefore exceeds the precision range of essentially any machine. Hence, by using a logarithmic transformation, the resulting values of (25.5) in the range of [0 1] are mapped by (25.6) into  $[-\infty 1]$ .

$$\begin{aligned} \text{Log}(P(Q, O | \lambda_L, \lambda_R, C)) &= \text{Log}(\pi_{q_L}) + \text{Log}(\pi_{q_R}) + \\ &\sum_{t=1}^T \text{Log}(a_{q_t, q_{t+1}L}) + \text{Log}(b_{q_tL}(o_t)) + \text{Log}(a_{q_t, q_{t+1}R}) + \text{Log}(b_{q_tR}(o_t)) + \text{Log}(c_{q_tLq_tR}) \end{aligned} \quad (25.6)$$

Due to the nature of the process associated with surgery in which the procedure, by definition, always starts at the idle state (state 1), the initial state distribution vector is defined as follows:

$$\begin{aligned} \pi_{1L} &= \pi_{1R} = 1 \\ \pi_{iL} &= \pi_{iR} = 0 \quad 2 \leq i \leq N \end{aligned} \quad (25.7)$$

Once the MMs were defined for specific subjects with specific skill levels, it became possible to calculate the statistical distance factors between them. These statistical distance factors are considered to be an objective criterion for

two potential transitions. However for simplifying the graphical representation of  $A = \{a_{ij}\}$  only one line is plotted between state  $i$  to state  $j$ . **(b)** Each state out of the 15 states of the left and the right tool  $b(L, R)_i$  is associated with the ten force/torque/velocity signature or discrete observation  $b_i(1) \dots b_i(10)$ . Each *line*, that connects the state with a specific observation represents probability value defined in observation symbol probability distribution matrix  $B = \{b_i(k)\}$ . The sub-structure appeared in (b) that is associated with each state was omitted for simplifying the diagram in (a)

evaluating skill level if for example the statistical distance factor between a trainee (indicated by index  $R$ ) and an expert (indicated by index  $E$ ) is being calculated. This distance indicates how similar is the performance of two subjects under study. Given two MMs  $\lambda_E$  (Expert) and  $\lambda_R$  (Novice) the nonsymmetrical statistical distances between them are defined as  $D_1(\lambda_R, \lambda_E)$  and  $D_2(\lambda_E, \lambda_R)$ . The natural expression of the symmetrical statistical distance version  $D_{ER}$  is defined by (25.8).

$$D_{ER} = \frac{D_1(O_E, Q_E, O_R, Q_R, \lambda_E) + D_2(O_E, Q_E, O_R, Q_R, \lambda_R)}{2} \quad (25.8)$$

$$= \left( \frac{\log P(O_R, Q_R | \lambda_E)}{\log P(O_E, Q_E | \lambda_E)} + \frac{\log P(O_R, Q_R | \lambda_R)}{\log P(O_E, Q_E | \lambda_R)} \right) / 2$$

Setting an expert level as the reference level of performance, the symmetrical statistical distance of a model representing a given subject from a given expert ( $D_{ER}$ ) is normalized with respect to the average distance between the models representing all the experts associated with the expert group ( $\bar{D}_{EE}$ ) and expressed in (25.9). The normalized distance  $\|D_{ER}\|$  represents how far (statistically) is the performance of a subject, given his or her model, from the performance of the average expert.

$$\|D_{ER}\| = \frac{D_{ER}}{\bar{D}_{EE}} = \frac{D_{ER}}{\frac{1}{l} \sum_{u=1;v=1}^{u=l;v=l} D_{E_u E_v}} \quad \text{for } u \neq v \quad (25.9)$$

For the purpose of calculating the normalized learning curve, the 20 distances between all the expert subjects was first calculated  $D_{E_u E_v}$  – (for five subjects in the expert group  $u = v = 1 \dots 5 - l = 20$ ) using (25.8). The denominator of (25.9) was then calculated. Once the reference level of expertise was determined, the statistical distances between each one of the 25 subjects, grouped into five levels of training (R1, R2, R3, R4, R5), and each one of the experts was calculated (five distances for each individual, 25 distances for each group of skill level and 125 distances for the entire data base) using (25.8). The average statistical distance and its variance defines the learning curve of a particular task.

#### 25.2.3.4 Complimentary Objective Indexes

In addition to the Markov models and the statistical similarity analysis, two other objective indexes of performance were measured and calculated, including the task completion time and the overall length ( $L$ ) of the path of the left and the right tool tips. Where  $d_L, d_R$  are the distances between two consecutive tool tip positions

$P_L(t-1), P_R(t-1)$  and  $P_L(t), P_R(t)$  as a function of time of the left and the right tools respectively.

$$L = \sum_{t=1}^T d_L(P_L(t-1), P_L(t)) + d_R(P_R(t-1), P_R(t)) \quad (25.10)$$

#### 25.2.4 Subjective Analysis: Scoring

The subjective performance analysis was based on an off-line unbiased expert surgeon review (blinded to the subject and training level of each individual) of digital videos recorded during the experiment. The review utilized a scoring system of four equally weighted criteria: (a) overall performance (b) economy of movement (c) tissue handling (d) number of errors including drop needle, drop suture, lose suture loop, breaking suture, needle injury to adjacent tissue, inability to puncture bowel with needle. Criteria (a), (b), and (c) included five levels. The final scores were normalized to the averaged experts scoring.

### 25.3 Results

#### 25.3.1 Force and Torque Position and Orientation

Typical raw data of forces and torques (F/T) and tool tip position were plotted using three dimensional graphs. The graphs show the kinematics and dynamics of the left and right endoscopic tools as measured by the Blue DRAGON while performing MIS intracorporeal knot by junior trainee (R1 – Fig. 25.5a, c) and expert surgeon (E – Fig. 25.5b, d). The F/T vectors can be depicted as arrows with origins located at the port, changing their lengths and orientations as a function of time and as a result of the F/T applied by the surgeon's hand on the tool. In a similar fashion, the traces of the tool tips with respect to the ports were plotted in Fig. 25.5c, d as their positions changed during the surgical procedure.

The forces along the Z axis (in/out of the port) were higher compared to the forces in the XY plane. On the other hand, torques developed by rotating the tool around the Z axis were extremely low compared to the torques generated while rotating the tool along the X and Y axis while sweeping the tissue or performing lateral retraction. Similar trends in terms of the F/T magnitude ratios between the X, Y, and Z axes were found in the data measured in other MIS tasks.

These raw data demonstrate the complexity of the surgical task and the multi-dimensional data associated with it. This complexity can be resolved in part by decomposing the surgical task into its primary elements enabling profound understanding of the MIS task.

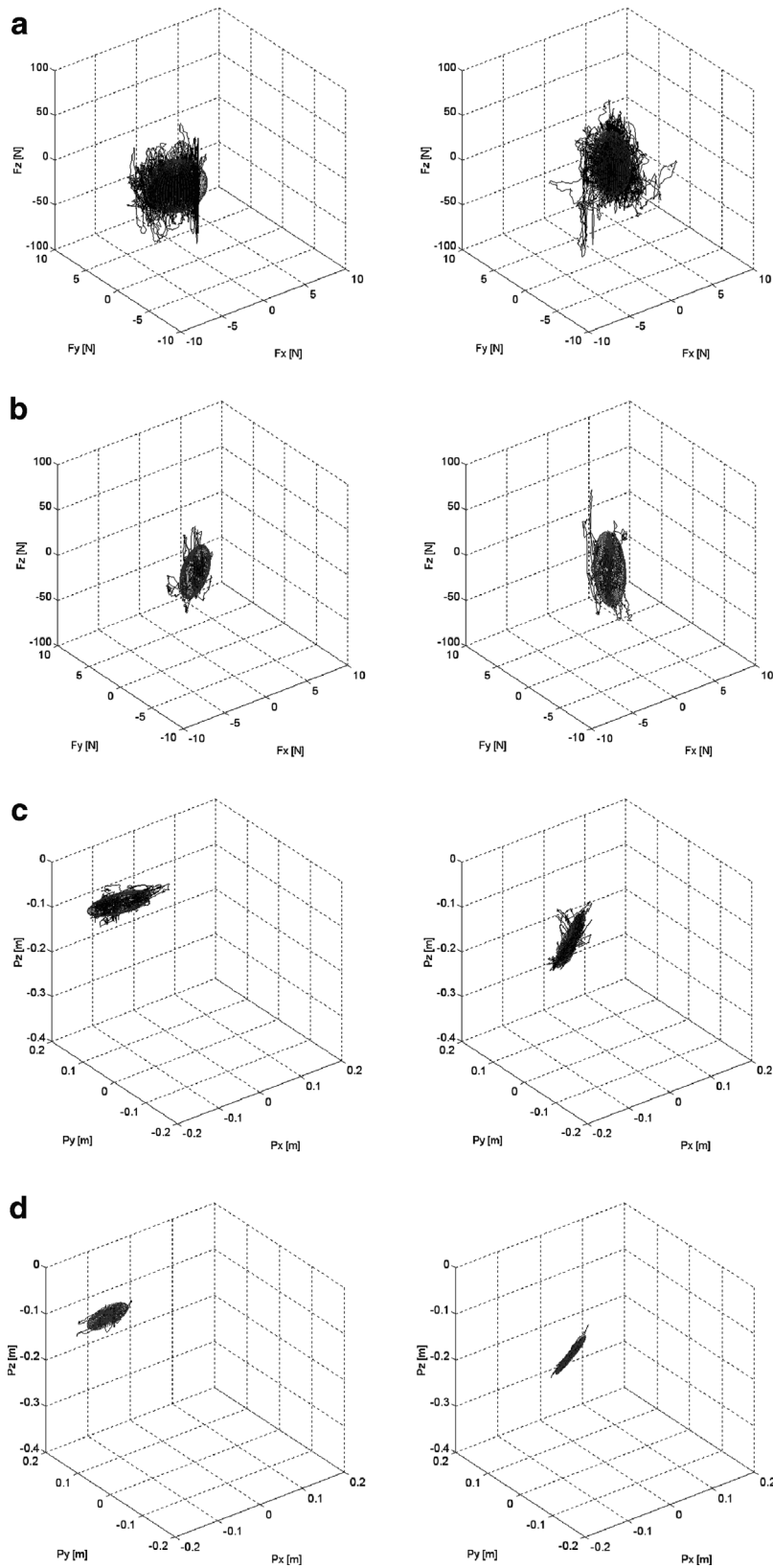


**Fig. 25.5** Kinematics and dynamic data from left and the right endoscopic tools measured by the Blue DRAGON while performing MIS suturing and knot tying by a trainee surgeon (**a, c**) and an expert surgeon (**b, d**) – (**a, b**) Forces; (**b, c**) tool tip position. The ellipsoids contain 95% of the data points

### 25.3.2 *Cluster Centers and Markov Models*

A cluster analysis using the K-means algorithm was performed to define typical cluster centers in the database. These were further used as code-words in the MM analysis. A total of 150 cluster centers were identified, ten clusters centers for each type of tool/tissue/object interaction as defined in Table 25.1. Figure 25.6 depicts the ten cluster centers associated with each one of the 15 states identified in the data. For example, Fig. 25.6 (13) represents ten cluster centers associated with the state defined by Grasping-Pushing-Sweeping (Table 25.1 – State No. 13). Grasping-Pushing-Sweeping is a superposition of three actions. The surgeon grasps a tissue or an object which is identified by the positive grasping force ( $F_g$ ) acting on the tool's jaws and the negative angular velocity of the handle ( $\omega_g$ ) indicating that the handle is being closed. At the same time the grasped tissue or object is pushed into the port indicated by positive value of the force ( $F_z$ ) acting along the long shaft of the tool and negative linear velocity ( $V_r$ ) representing the fact the tool is moved into the port. Simultaneously, sweeping the tissue to the side manifested by the force and the torque in the XY plane ( $F_{xy}, T_{xy}$ ) that are generated due to the deflection of the abdominal wall, the lateral force applied on the tool by the tissue or object being swept along with the lateral angular velocity ( $\omega_{xy}$ ) indicating the rotation of the tool around the pivot point inside the port.

Both static, quasi-static and dynamic tool/tissue or tool/object interactions are represented by the various cluster centers. Even in static conditions, the forces and torques provide a unique and un-ambivalent signature that can be associated with each one of the 15 states.

The 150 cluster centers (Table 25.1 and Fig. 25.6) form a code-book that is used to encode the entire database of the actual surgical procedure converting the continuous multi-dimensional data into a one-dimensional vector of finite symbols. It should be noted that since each state is associated with a unique set of ten cluster centers and vice versa, a specific cluster center was associated with only one state, and as a by-product of the encoding process, the states were also identified.

### 25.3.3 *Objective and Subjective Indexes of Performance*

Given the encoded data, the MM for each subject was calculated defining the probabilities for performing certain tool transitions ( $[A]$  matrix), the probability of combining two states ( $[C]$  matrix), and the probability of using the various signatures in each state ( $[B]$  matrix) – Fig. 25.7. The highest probability values in the  $[A]$  matrix usually appeared along the diagonal. These results indicate that a transition associated with staying at the same state is more likely to occur rather than a transition to any one of the other 15 potential states. In minimally invasive surgical suturing, the default transition between any state is to the grasping state (state number 2) as indicated by the high probability values along the second column of the  $[A]$  matrix. Probability of using one out of the 150 cluster centers defined in Fig. 25.7 is graphically represented by the  $[B]$  matrix. Each line of the  $[B]$  matrix is

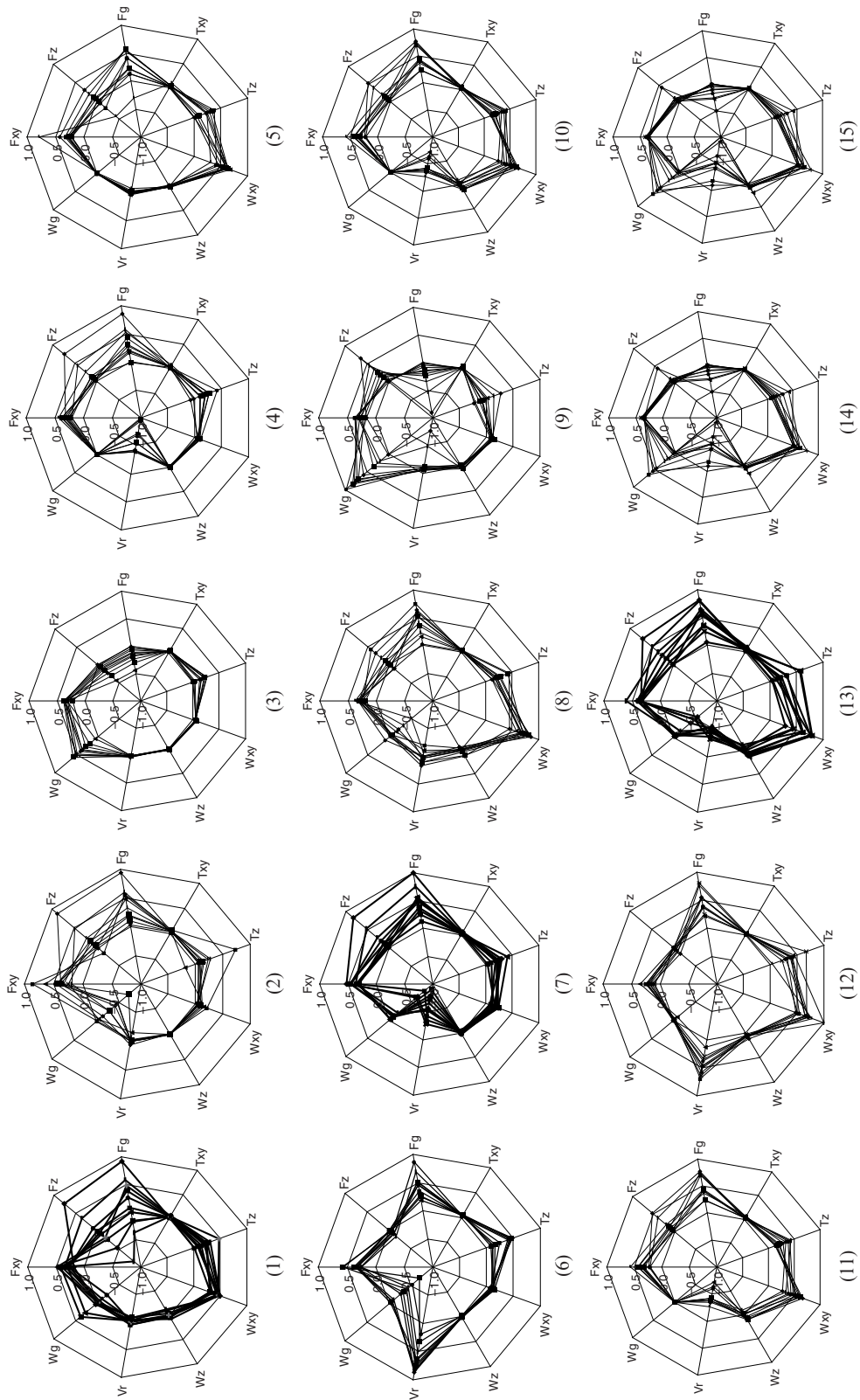


**Fig. 25.6** Cluster centers definition – Ten signatures of forces torques linear and angular velocities associated with the 15 types of states (tool/tissue or tool/object interaction) defined by Table 25.1. In these graphs each one of the ten polar lines represent one cluster. The clusters were normalized to a range of  $[-1 \ 1]$  using the following min/max values:  $\omega_{xy} = 0.593[\text{r/s}]$ ,  $\omega_z = 2.310[\text{r/s}]$ ,  $V_r = 0.059[\text{m/s}]$ ,  $\omega_g = 0.532[\text{r/s}]$ ,  $F_{xy} = 5.069[\text{N}]$ ,  $F_z = 152.536[\text{N}]$ ,  $F_g = 33.669[\text{N}]$ ,  $T_{xy} = 9.792[\text{Nm}]$ ,  $T_z = 0.017[\text{Nm}]$ . The numbers correspond to the 15 states as defined by Table 25.1

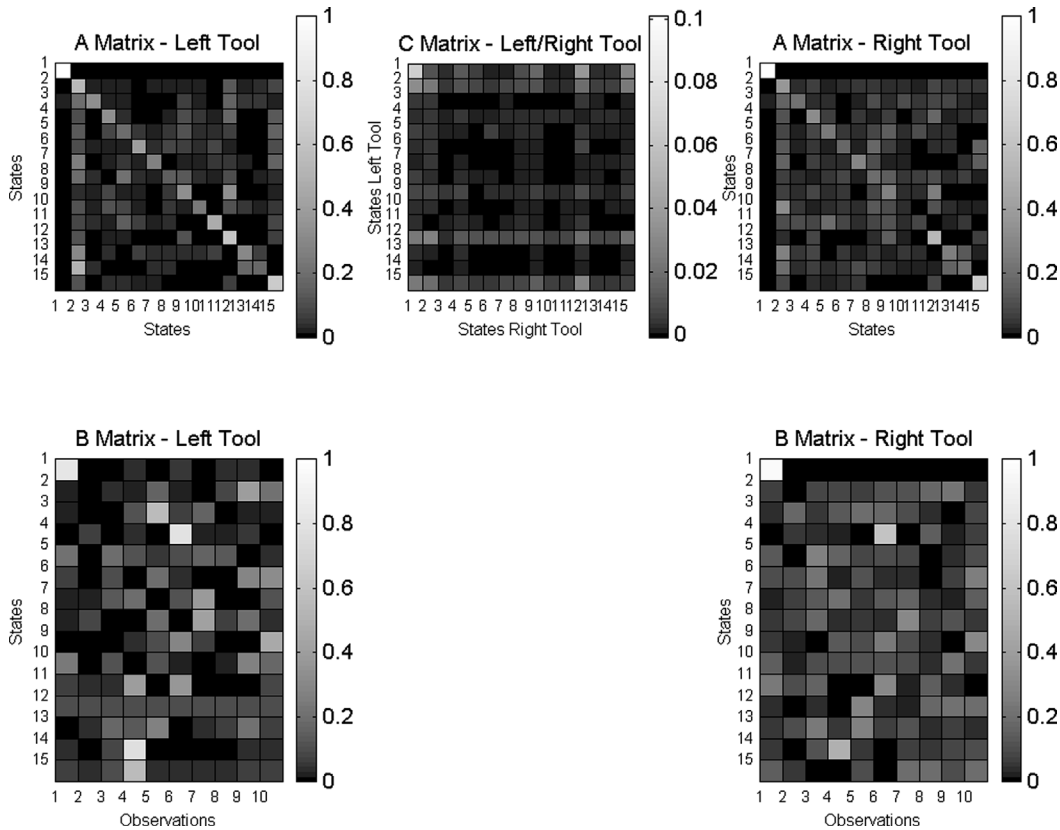


**Fig. 25.7** A typical Markov Model where the matrices  $[A]$ ,  $[B]$ ,  $[C]$ , are represented as color-coded probabilistic maps

associated with one of the ten states. The clusters were ranked according to the mechanical power. The left and the right tool used different distribution of the clusters. Whereas with the left tool the most frequent clusters that were used are related to mid-range power with the right tool the cluster usage is more evenly distributed among the different power levels. The collaboration matrix  $[C]$  indicates that the most frequently used state with both the left and the right tools are idle (state 1), grasping (state 2) grasping pulling and sweeping (state 12) and grasping rotating (state 15) with the left tool. Once one of the tools utilizes one of these states, the probability of using any of the states by the other tool is equally distributed between the states which is indicated by the bright horizontal stripes in the graphical representation of the  $[C]$  matrix.

The Idle state (state 1) in which no tool/tissue interaction is performed, was mainly used by both expert and novice surgeons, to move from one operative state to the another. However, the expert surgeons used the idle state only as a transition state while the novices spent a significant amount of time in this state planning the next tool/tissue or tool/object interaction. However, in case of surgical suturing and knot tying, the grasping state (state 2) dominated the transition phases since grasping state maintained the operative state in which both the suture and the needle were held by the two surgical tools.

Figure 25.8a–c represent the normalized MM-based statistical distance as a function of the training level, the normalized completion time, and the normalized path length of the two tool tips respectively. The subjective normalized scoring is

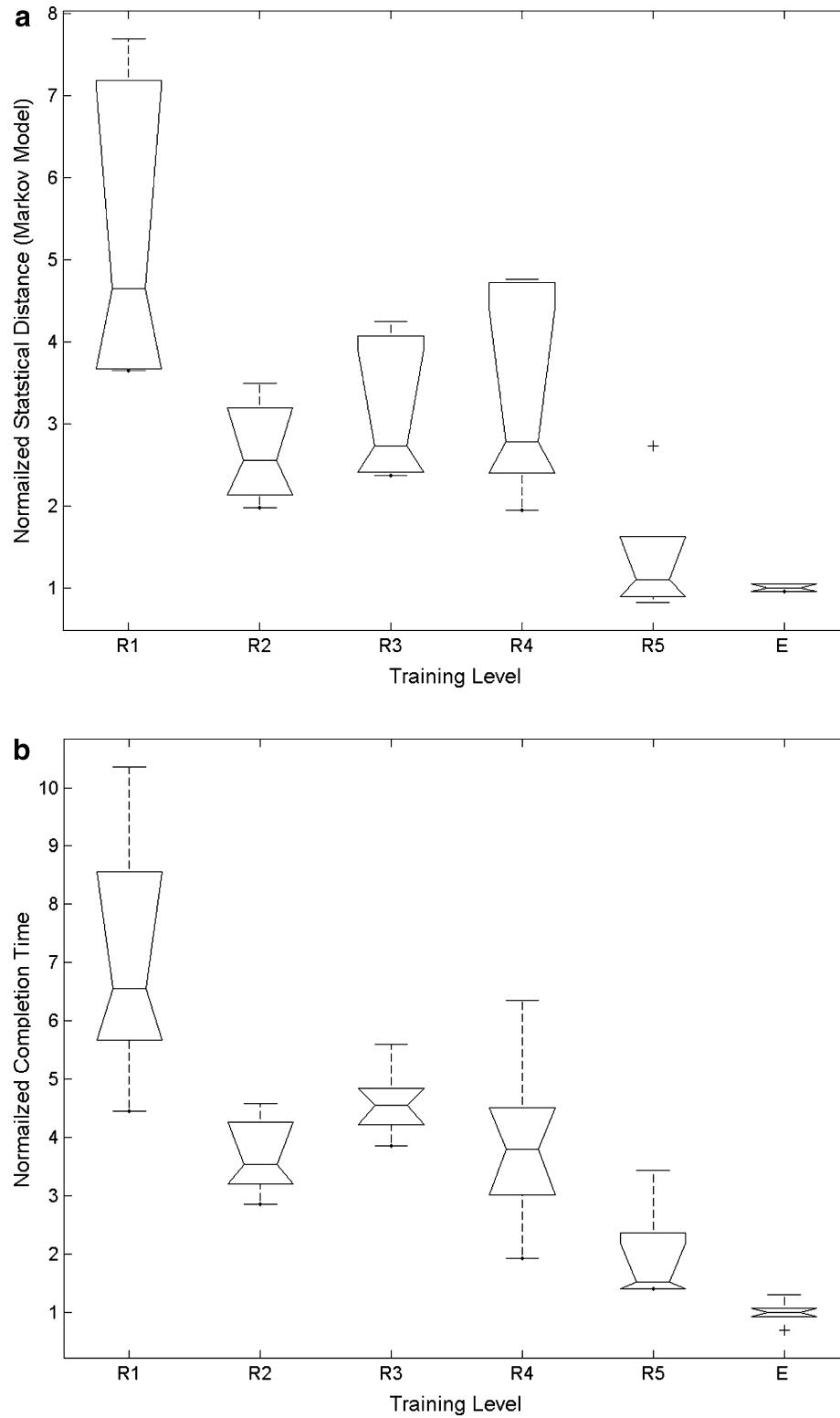


**Fig. 25.8** Objective and subjective assessment indexes of minimally invasive suturing learning cure. The objective performance indexes are based on: (a) Markov model normalized statistical distance, (b) normalized completion time, and

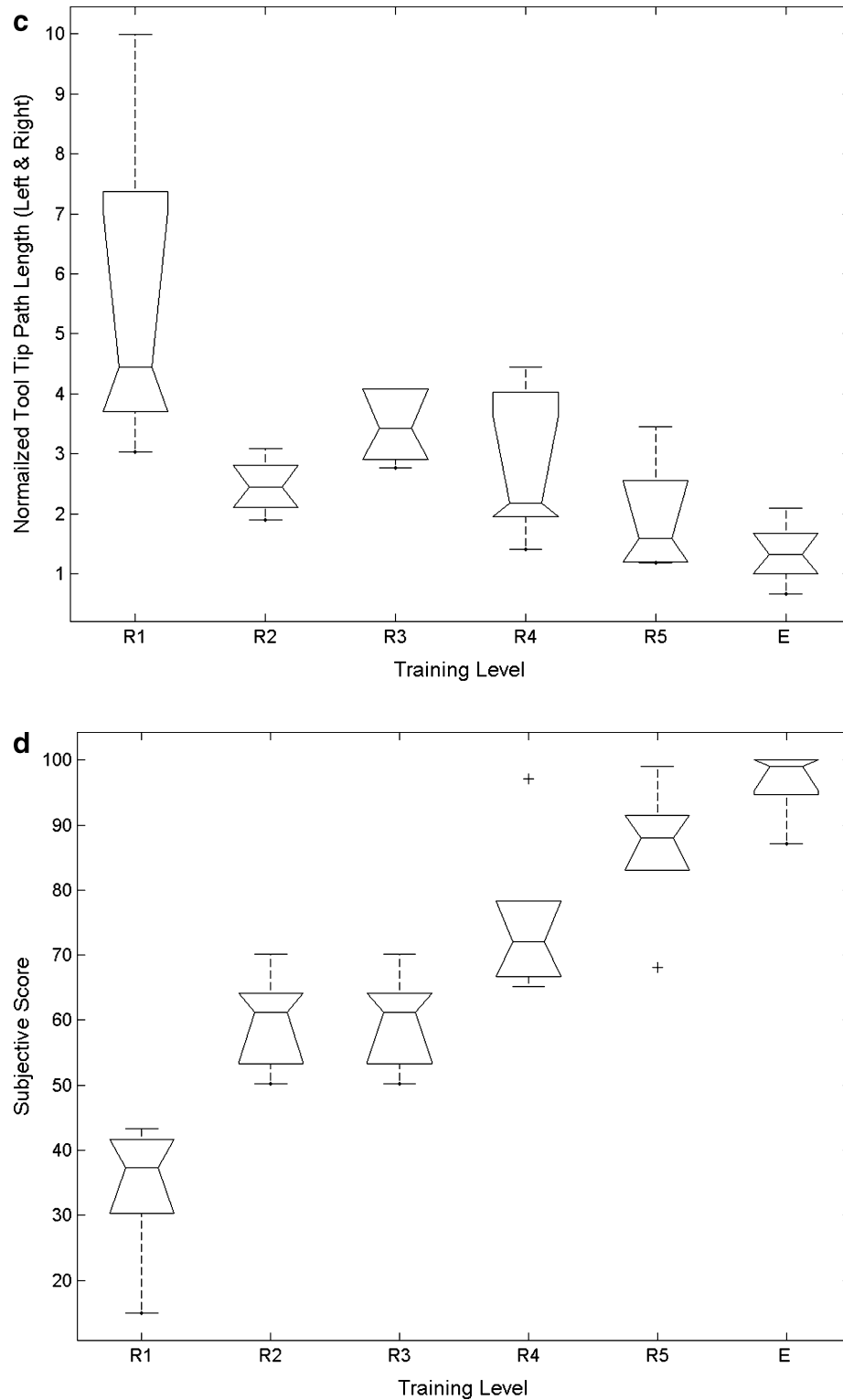


**Fig. 25.8** (continued) (c) normalized path length of the two tool tips. The average task completion time of the expert group is 98 s and the total path length of the two tools is 3.832 m. The subjective performance index is based on visual scoring by an expert surgeon normalized with respect to experts' performance (d)

depicted in Fig. 25.8d. The data demonstrate that substantial suturing skills are acquired during the first year of the residency training. The learning curves do not indicate any significant improvement during the second and the third years of training. The rapid improvement of the first year is followed by lower gradient of the learning curve as the trainees progress toward the expert level. However, the MM based statistical distance along with the completion time criteria show yet another gradient in the learning curve that occurs during the fourth year of the residency training followed by slow conversion to expert performance. Similar trends in the learning curve are also demonstrated by the subjective assessment. One of the subjects in the R2 group outperformed his peers in his own group and some subjects in a more advanced groups (R3, R4). Although, statistically insignificant, the performance slightly altered the overall trend of the learning curves as defined by the different criteria.

A correlation analysis was performed between the means of the objective normalized MM based statistical distance and the subjective normalized scoring. The correlation factor  $R^2$  was found to be 0.86. This result established the linkage between objective and subjective methodologies for assessing surgical skill (Fig. 25.9).

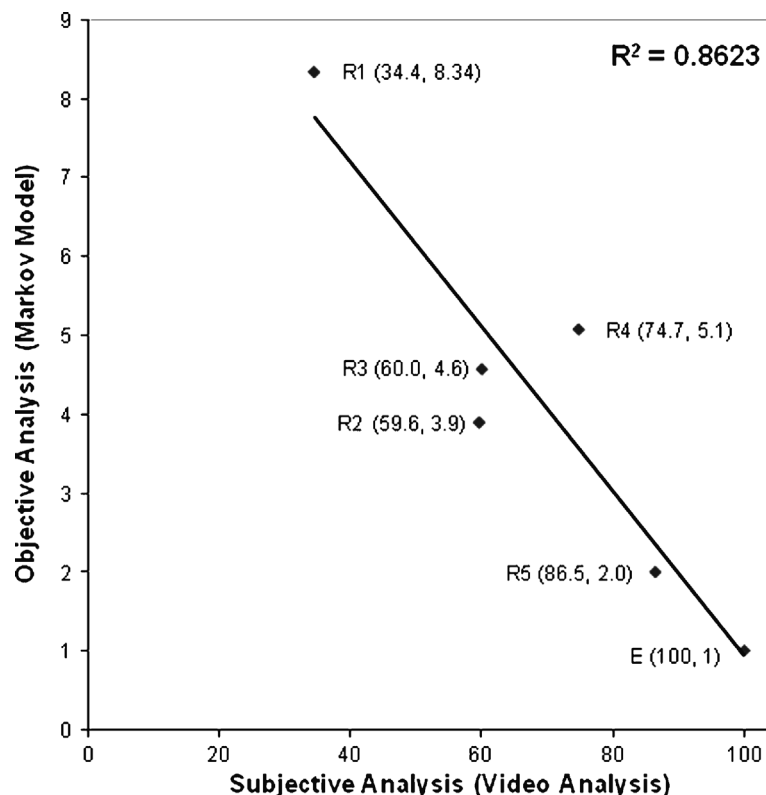


**Fig. 25.9** Linear correlation between the normalized mean performance obtained by a subjective video analysis and objective analysis using Markov models and the statistical distance between models of trainees (R1–R5) and experts (E). The notations R1, R2, R3, R4, R5 represent the various residence groups where the number denotes year of training and E indicate expert surgeons. The *values* in the *brackets* represent the normalized mean scores using the subjective and the objective methodologies respectively

Detailed analysis of the MM shows that major differences between surgeons at different skill levels were: (a) the types of tool/tissue/object interactions being used, (b) the transitions between tool/tissue/object interactions being applied by each hand, (c) time spent while performing each tool/tissue/object interaction, (d) the overall completion time, (e) the various F/T/velocity magnitudes being applied by the subjects through the endoscopic tools, and (f) two-handed collaboration. Moreover, the F/T associated with each state showed that the F/T magnitudes were found to be task-dependent. High F/T magnitudes were applied by novices compared to experts during tissue manipulation, and vice versa during tissue dissection. High efficiency of surgical performance was demonstrated by the expert surgeons and expressed by shorter tool tip displacements, shorter periods of time spent in the 'idle' state, and sufficient application of F/T on the tissue to safely accomplish the task.

## 25.4 Discussion

Minimally invasive surgery, regardless of the performance modality, is a complex task that requires synthesis between visual and kinesthetic information. Analyzing MIS in terms of these two sources of information is a key step towards developing objective criteria for training surgeons and evaluating the performance in different modalities including real surgery, master/slave robotic systems or virtual reality simulators with haptic technology.

Following two steps of data reduction, data that was collected by the Blue DRAGON were further used to develop models representing MIS as a process. In any data reduction there is always a compromise between decreasing the input dimensionality while retaining sufficient information to characterize and model the process under study. Utilizing the VQ algorithm the 13 dimensional stream of acquired data were quantized into 150 symbols with nine dimensions each.

The data quantization included two substeps. In the first steps the cluster centers were identified. As part of the second step the entire database was encoded based on the cluster centers defined in the first step. Every data point needs to meet two criteria in order to be associated with one of the 150 cluster centers defined in the first step. The first criterion is to have the minimal geometrical distance to one of the cluster centers. Once the data point was associated with a specific cluster center it is by definition associated with a specific state out the 15 defined. Based on expert knowledge of surgery, Table 25.1 defines the 15 states and unique sets of individual vector components. The second criterion is that given the candidate state and the data vector, the direction of each component in the vector must match the one defined by the table for the selected state. It was indicated during the data processing that these two criteria were always met suggesting that the data quantization process is very robust in its nature. Following the encoding process a 2 dimensional input (one dimension for each tool) was utilized to form a 30 state fully connected Markov model. The coded data with their close association to the measured data, as well as the Markov model using these codes as its observations distributed among

its states, retain sufficient multi model information in a compact mathematical formulation for modeling the process of surgery at different levels.

MIS is recognized both qualitatively and quantitatively as multidimensional process. As such, studying one parameter e.g. completion time, tool-tip paths, or force/torque magnitudes reveals only one aspect of the process. Only a model that truly describes MIS as a process is capable of exposing the process internal dynamics and provides wide spectrum information about it. At the high level, a tremendous amount of information is encapsulated into a single objective indicator of surgical skill level and expressed as the statistical distance between the surgical performance of a particular subject under study from a surgical performance of an expert. As part of an alternative approach a combined score could be calculated by studying each parameter individually (e.g. force, torque, velocity, tool path, completion time etc.), assigning a weight to each one of these parameters, which is a subjective process by itself, and combining them into a single score. The assumption underlying this approach is that a collection of aspects associated with surgery may be used to assess the overall process. However this alternative approach ignores the internal dynamics of the process that is more likely to be revealed by a model such as the Markov model. In addition, as opposed to analyzing individual parameters, studying the low levels of the model provides profound insight into the process of MIS in a way that allows one to offer constructive feedback for a trainee regarding performance aspects like the appropriate application of F/T, economy of motion, and two handed manipulation.

The appropriate application of F/T on the tissue has a significant impact on the surgical performance efficiency and outcome of surgery. Previous results indicated that the F/T magnitudes are task dependent [3–7]. Experts applied high F/T magnitudes on the tissues during tissue dissection as opposed to low F/T magnitudes applied on the tissues by trainees that were trying to avoid irreversible damage. An inverse relationship regarding the F/T magnitudes was observed during tissue manipulation in which high F/T magnitudes applied on the tissue by trainees exposed them to acute damage. It is important to point out that these differences were observed in particular states (e.g. all the states including grasping for tissue manipulation and all the state that involved spreading for tissue dissection). Due to the inherent variance in the data even multidimensional ANOVA failed to identify this phenomena once the F/T magnitudes are removed from the context of the multi state model. Given the nature of surgical task, the Markov model [B] Matrix, encompassing information regarding the frequency in which the F/T magnitudes were applied, may be used to assess whether the appropriate magnitudes F/T were applied for each particular state. For obvious reasons, tissue damage is correlated with surgical outcome, and linked to the magnitudes and the directions in which F/T were applied on the tissues. As such, tissue damage boundaries may be incorporated into the [B] matrix for each particular state. Given the surgical task, this additional information may refine the contractive feedback to the trainee and the objective assessment of the performance.

The economy of motion and the two hand collaboration may be further assessed by retrieving the information encapsulated into the [A], and [C] matrices. The

amount of information incorporated into these two data structures is well beyond the information provided by a single indicator such as tool-tip path length, or completion time for the purpose of formulating constructive feedback to the trainee. Given a surgical task, utilizing the appropriate sets of states and state transitions are skill dependent. This information is encompassed in the [A] matrix indicating that states that were in use and the state transitions that were performed. Moreover, the ability to refine the time domain analysis using the multi state Markov model indicated, as was observed in previous studies, that the 'idle' state is utilized as a transition state by expert surgeons whereas a significant amount of time is spent in that state by trainees [3–7]. In addition, coordinated movements of the two tools is yet another indication of high skill leveling MIS. At a lower skill level the dominant hand is more active than the non-dominant hand as opposed to a high skill level in which the two tools are utilized equally. The collaborated [C] matrix encapsulates this information and quantifies the level of collaboration between the two tools.

In conclusion, the MM model provides insight into the process of performing MIS. This information can be translated into a constructive feedback to the trainee as indicated by the model three matrices [A], [B] and [C]. Moreover, the capability of running the model in real-time and its inherent memory allows a senior surgeon supervising the surgery or an artificial intelligent expert system incorporated into a surgical robot or a simulator provides an immediate constructive feedback during the process as previously described.

A useful analogy of the proposed methodology for decomposing the surgical task is the human spoken language. Based on this analogy, the basic states – tool/tissue interactions are equivalent to 'words' of the MIS 'language' and the 15 states form the MIS 'dictionary' or set of all available words. In the same way that a single word can be pronounced differently by various people, the same tool/tissue or tool/object interaction can be performed differently by different surgeons. Differences in F/T magnitudes account for this different 'pronunciation', yet different pronunciation of a 'word' have the same meaning, or outcome, as in the realm of surgery. The cluster analysis was used to identify the typical F/T and velocities associated with each one of the tool/tissue and tool/object interactions in the surgery 'dictionary', or using the language analogy, to characterize different pronunciations of a 'word'. Utilizing the 'dictionary' of surgery, the MM was then used to define the process of each task or step of the surgical procedure, or in other words, 'dictating chapters' of the surgical 'story'. This analogy is reinforced by an important finding in the field of Phonology suggesting that all human languages use a limited repertoire of about 40–50 sounds defined as phones [45] e.g. the DARPA phonetic alphabet, ARPAbet used in American English or the International Phonetic Alphabet (IPA). The proposed methodology retains its power by decomposing the surgical task to its fundamental elements – tool/tissue and tool/object interactions. These elements are inherent in MIS no matter which modality is being used.

One may note that although the notations and the model architecture of the proposed Markov model (MM) and the hidden Markov model (HMM) approach are similar, there are several fundamental differences between them. Strictly speaking, the proposed MM is a *white box* model in which each state has a physical meaning

describing a particular interaction between the tools and tissue or other objects in the surgical scene like sutures and needles. However, the HMM is a *black box* model in which the states are abstract and are not related to a specific physical interaction. Moreover, in the proposed white box model, each state has a unique set of observations that characterize only the specific state. By definition, once the discrete observation is matched with a vector quantization code-word the state is also defined. States in the HMM share the same observations, however different observation distributions differentiate between them. The topology of the proposed MM suggests a hybrid approach between the two previously described models. It adds to the classic Markov model another layer of complexity by introducing the observation elements for each state. The model also provides insight into the process by linking the states to physical and meaningful interactions. This unique quality adds to the classic notation of the introduction of the collaboration matrix  $[C]$ . This matrix is not present in either the MM or the HMM. The  $[C]$  matrix was introduced as a way to link between the models representing the left and right hand tools since surgery is a two-handed task.

Quantifying the advantages and the disadvantages of each modeling approach (MM or HMM) is still a subject for active research. Whereas the strength of the MM is expressed by providing physical meaning to the process being modeled, development of HMM holds the promise for more compact model topology which avoids any expert knowledge incorporated into the model. Regardless of the type of the model, defining the scope of the model and its fundamental elements, the state and the observation are subjects of extensive research. In the current study the entire surgical task is modeled by a fully connected model topology where each tool/tissue/object interaction is modeled as a state. In a different approach, using a state of the art methodology in speech recognition in which each phenomenon is represented by a model with abstract states, each tool/object interaction is modeled by entire model using more generalized definitions for these interactions e.g. place position, insert remove [46, 47]. This approach may require additional model with a predetermined overall structure that will represent the overall process.

The scope of the proposed model is limited to objectively assess technical factors of surgical ability. Cognitive factors per se cannot be assessed by the model unless a specific action is taken as a result of a decision making process. In any case, the model is incapable of tracing the process back to its cognitive origin. In addition, the underlying assumption made by using a model is that there is a standard technique with insignificant variations by which expert surgeons perform a surgical task. Any significant variation of the surgical performance, regardless of the surgical outcome, is penalized by the model and associated with low scores. If such a surgical performance variation from the standard surgical technique is associated with a better outcome for the patient the model is incapable of detecting it.

Decomposing MIS and analyzing it using MM is one approach for developing objective criteria for surgical performance. The availability of validated objective measures of surgical performance and competency is considered critical for training surgeons and evaluating their performance. Systems like surgical robots or virtual reality simulators that inherently measure the kinematics and the dynamics of the

surgical tools may benefit from inclusion of the proposed methodology. Using this information in real-time during the course of learning as feedback to the trainee surgeons or as an artificial intelligent background layer, may increase performance efficiency in MIS and improve patient safety and outcome.

## References

1. Satava, R.: Metrics for Objective Assessment of Surgical Skills Workshop – Developing Quantitative Measurements through Surgical Simulation. Scottsdale, Arizona (2001)
2. Gallagher, A.G., Satava, R.M.: Virtual reality as a metric for the assessment of laparoscopic psychomotor skills. Learning curves and reliability measures. *Surg Endosc.* **16**(12), 1746–1752 (2002)
3. Rosen, J., Hannaford, B., Richards C., Sinanan, M.: Markov modeling of minimally invasive surgery based on tool/tissue interaction and force/torque signatures for evaluating surgical skills. *IEEE Trans. Biomed. Eng.* **48**(5), 579–591 (2001)
4. Richards, C., Rosen, J., Hannaford, B., MacFarlane, M., Pellegrini, C., Sinanan, M.: Skills evaluation in minimally invasive surgery using force/torque signatures. *Surg. Endosc.* **14**(9), 791–798 (2000)
5. Rosen J., Solazzo, M., Hannaford, B., Sinanan, M.: Objective evaluation of laparoscopic skills based on haptic information and tool/tissue interactions. *Comput. Aided Surg.* **7**(1), 49–61 (2002)
6. Rosen J., Brown, J.D., Barreca, M., Chang, L., Hannaford, B., Sinanan, M.: The blue DRAGON, a system for monitoring the kinematics and the dynamics of endoscopic tools in minimally invasive surgery for objective laparoscopic skill assessment. In: Proceedings of MMVR 2002. IOS Press, Amsterdam (2002)
7. Rosen, J., Brown, J.D., Chang, L., Barreca, M., Sinanan, M., Hannaford, B.: The blue DRAGON – a system for measuring the kinematics and the dynamics of minimally invasive surgical tools in-vivo. In: Proceedings of the 2002 IEEE International Conference on Robotics & Automation, Washington DC, USA, 11–15 May 2002
8. McBeth, P.B., Hodgson, A.J., Nagy, A.G., Qayumi, K.: Quantitative methodology of evaluating surgeon performance in laparoscopic surgery. In: Proceedings of MMVR 2002. IOS Press, Amsterdam (2002)
9. Ibbotson, J.A., MacKenzie, C.L., Cao, C.G.L., Lomax, A.J.: Gaze patterns in laparoscopic surgery. In: Westwood, J.D., Hoffman, H.M., Robb, R.A., Stredney, D. (eds.) *Medicine Meets Virtual Reality*, vol. 7, pp. 154–160. IOS Press, Washington, DC (1999)
10. Pugh, C.M., Youngblood, P.: Development and validation of assessment measures for a newly developed physical examination simulator. *J. Am. Med. Inform. Assoc.* **9**(5), 448–460 (2002)
11. Noar, M.: Endoscopy simulation: a brave new world? *Endoscopy* **23**, 147–149 (1991)
12. Satava, R.: Virtual reality surgical simulator. *Surg. Endosc.* **7**, 203–205 (1993)
13. Ota, D., Loftin, B., Saito, T., Lea, R., Keller, J.: Virtual reality in surgical education. *Comput. Biol. Med.* **25**, 127–137 (1995)
14. Berkely, J., Weghorst, S., Gladstone, H., Raugi, G., Ganter, M., Fast Finite Element Modeling for Surgical Simulation, Proceedings. *Stud. Health Technol. Inform.* **62**, 55–61 (1999)
15. Tseng, C.S., Lee, Y.Y., Chan, Y.P., Wu, S.S., Chiu, A.W.: A PC-based surgical simulator for laparoscopic surgery. *Stud. Health Technol. Inform.* **50**, 155–160 (1998)
16. Delingette, H., Cotin, S., Ayache, N.: Efficient linear elastic models of soft tissues for real-time surgery simulation. *Stud. Health Technol. Inform.* **62**, 100–101 (1999)
17. Basdogan, C., Ho, C.H., Srinivasan, M.A.: Simulation of tissue cutting and bleeding for laparoscopic surgery using auxiliary surfaces. *Stud. Health Technol. Inform.* **62**, 38–44 (1999)

18. Acosta, E., Temkin, B., Krummel, T.M., Heinrichs, W.L.: G2H—graphics-to-haptic virtual environment development tool for PC's. *Stud. Health Technol. Inform.* **70**, 1–3 (2000)
19. Akatsuka, Y., Shibasaki, T., Saito, A., Kosaka, A., Matsuzaki, H., Asano, T., Furuhashi, Y.: Navigation system for neurosurgery with PC platform. *Stud. Health Technol. Inform.* **70**, 10–16 (2000)
20. Berkley, J., Oppenheimer, P., Weghorst, S., Berg, D., Raugi, G., Haynor, D., Ganter, M., Brooking, C., Turkiyyah, G.: Creating fast finite element models from medical images. *Stud. Health Technol. Inform.* **70**, 26–32 (2000)
21. el-Khalili, N., Brodlie, K., Kessel, D.: WebSTER: a web-based surgical training system. *Stud. Health Technol. Inform.* **70**, 69–75 (2000)
22. Friedl, R., Preisack, M., Schefer, M., Klas, W., Tremper, J., Rose, T., Bay, J., Albers, J., Engels, P., Guilliard, P., Vahl, C.F., Hannekum, A.: CardioOp: an integrated approach to teleteaching in cardiac surgery. *Stud. Health Technol. Inform.* **70**, 76–82 (2000)
23. Gobbetti, E., Tuveri, M., Zanetti, G., Zorcolo, A.: Catheter insertion simulation with co-registered direct volume rendering and haptic feedback. *Stud. Health Technol. Inform.* **70**, 96–98 (2000)
24. Gorman, P., Krummel, T., Webster, R., Smith, M., Hutchens, D.: A prototype haptic lumbar puncture simulator. *Stud. Health Technol. Inform.* **70**, 106–109 (2000)
25. Anne-Claire, J., Denis, Q., Patrick, D., Christophe, C., Philippe, M., Sylvain, K., Carmen, G.: S.P.I.C. pedagogical simulator for gynecologic laparoscopy. *Stud. Health Technol. Inform.* **70**, 139–145 (2000)
26. Tasto, J.L., Verstreken, K., Brown, J.M., Bauer, J.J.: PreOp endoscopy simulator: from bronchoscopy to ureteroscopy. *Stud. Health Technol. Inform.* **70**, 334–349 (2000)
27. Wiet, G.J., Stredney, D., Sessanna, D., Bryan, J.A., Welling, D.B., Schmalbrock, P.: Virtual temporal bone dissection: an interactive surgical simulator. *Otolaryngol. Head Neck Surg.* **127** (1), 79–83 (2002)
28. John, N.W., Thacker, N., Pokric, M., Jackson, A., Zanetti, G., Gobbetti, E., Giachetti, A., Stone, R.J., Campos, J., Emmen, A., Schwerdtner, A., Neri, E., Franceschini, S.S., Rubio, F.: An integrated simulator for surgery of the petrous bone. *Stud. Health Technol. Inform.* **81**, 218–224 (2001)
29. Bielser, D., Gross, M.H.: Open surgery simulation. *Stud. Health Technol. Inform.* **81**, 57–63 (2001)
30. Berg, D., Berkley, J., Weghorst, S., Raugi, G., Turkiyyah, G., Ganter, M., Quintanilla, F., Oppenheimer, P.: Issues in validation of a dermatologic surgery simulator. *Stud. Health Technol. Inform.* **81**, 60–65 (2001)
31. Manyak, M.J., Santangelo, K., Hahn, J., Kaufman, R., Carleton, T., Hua, X.C., Walsh, R.J.: Virtual reality surgical simulation for lower urinary tract endoscopy and procedures. *J. Endourol.* **16**(3), 185–190 (2002)
32. Basdogan, C., Ho, C., Srinivasan, M.A.: Virtual environments for medical training: graphical and haptic simulation of common bile duct exploration (PDF). *IEEE/ASME Trans. Mechatron. (special issue on Haptic Displays and Applications)* **6**(3), 267–285 (2001)
33. Cao, C.G.L., MacKenzie, C.L., Ibbotson, J.A., Turner, L.J., Blair, N.P., Nagy, A.G.: Hierarchical decomposition of laparoscopic procedures. In: Westwood, J.D., Hoffman, H.M., Robb, R.A., Stredney, D. (eds.) *Medicine Meets Virtual Reality*, vol. 7, pp. 83–89. IOS Press, Washington, DC (1999)
34. M.C., Villanueva, I., Tendick, F.: Workspace analysis of robotic manipulator for teleoperated suturing task. In: *Proceeding of IEEE/IROS, Maui Hawaii, USA* (2001)
35. Rabiner, L.R.: A tutorial on hidden Markov models and selected application in speech recognition. *Proc. IEEE* **77**(2) (1989)
36. Hannaford, B., Lee, P.: Hidden Markov model of force torque information in telemanipulation. *Int. J. Robot. Res.* **10**(5), 528–539 (1991)
37. Pook, P., Ballard, D.H.: Recognizing teleoperated manipulations. In: *Proc. IEEE Robotics and Automation*, vol. 2, pp. 578–585, Atlanta, GA, May 1993

38. Nechyba, M.C., Xu, Y.: Stochastic similarity for validating human control strategy models. *IEEE Trans. Robot. Autom.* **14**(3), 437–451 (1998)
39. Yang, J., Xu, Y., Chen, C.-S.: Human action learning via hidden Markov model. *IEEE Trans. Syst. Man Cybern. A (Syst. Hum.)* **27**(1), 34–44 (1997)
40. Itabashi, K., Hirana, K., Suzuki, T., Okuma, S., Fujiwara, F.: Modeling and realization of the peg-in-hole task based on hidden Markov model. In: *Proc. IEEE Intl. Conf. on Robotics and Automation*, Leuven, Belgium, pp. 1142, May 1998
41. Wachsmuth I, Frohlich M. (eds.) *Gesture and Sign Language in Human–Computer Interaction*, International Gesture Workshop Proceedings, xi+308 pp. Springer, Berlin, Germany (1998)
42. Lien, J.J., Kanade, T., Cohn, J.F., Li, C.C.: Automated facial expression recognition based on FACS action units. In: *Proceedings Third IEEE International Conference on Automatic Face and Gesture Recognition (Cat. No.98EX107)*, Nara, Japan, pp. 390–395, 14–16 April 1998
43. Baldi, P., Brunak S.: *Bioinformatics*. MIT Press, Cambridge, MA (1998)
44. Murphy, T.E., Vignes, C.M., Yuh, D.D., Okamura, A.M.: Automatic Motion Recognition and Skill Evaluation for Dynamic Tasks. In: *Eurohaptics* (2003)
45. Russell, S.J., Norvig, P.: *Artificial Intelligence – A Modern Approach*, 2nd edn. Pearson Education, Inc., Upper Saddle River, NJ (2003)
46. Li, M., Okamura, A.M.: Recognition of operator motions for real-time assistance using virtual fixtures. In: *11th International Symposium on Haptic Interfaces for Virtual Environment and Teleoperator Systems, IEEE Virtual Reality*, pp. 125–131 (2003)
47. Hundtofte, C.S., Hager, G.D., Okamura, A.M.: Building a task language for segmentation and recognition of user input to cooperative manipulation systems. In: *10th International Symposium on Haptic Interfaces for Virtual Environment and Teleoperator Systems*, pp. 225–230 (2002)
48. Bow, S.T.: *Pattern Recognition*. Marcel, Dekker Inc., New York (1984)